Accepted Manuscript

Discovery of 1,2,4-oxadiazole-Containing hydroxamic acid derivatives as histone deacetylase inhibitors potential application in cancer therapy

Zhuang Yang, Mingsheng Shen, Minghai Tang, Wanhua Zhang, Xue Cui, Zihao Zhang, Heying Pei, Yong Li, Mengshi Hu, Peng Bai, Lijuan Chen

PII: S0223-5234(19)30513-6

DOI: https://doi.org/10.1016/j.ejmech.2019.05.089

Reference: EJMECH 11399

To appear in: *European Journal of Medicinal Chemistry*

Received Date: 16 February 2019

Revised Date: 18 May 2019

Accepted Date: 31 May 2019

Please cite this article as: Z. Yang, M. Shen, M. Tang, W. Zhang, X. Cui, Z. Zhang, H. Pei, Y. Li, M. Hu, P. Bai, L. Chen, Discovery of 1,2,4-oxadiazole-Containing hydroxamic acid derivatives as histone deacetylase inhibitors potential application in cancer therapy, *European Journal of Medicinal Chemistry* (2019), doi: https://doi.org/10.1016/j.ejmech.2019.05.089.

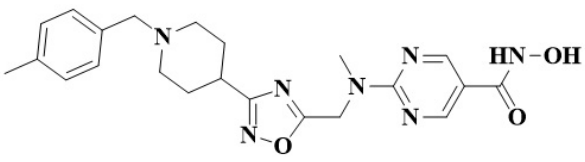

14b

HDAC1 = 1.8 ± 0.2 nM; HDAC2 = 3.6 ± 0.3 nM
HDAC3 = 3.0 ± 0.8 nM
Antiproliferative IC_{50}s = 10-45 nM
***F* = 53.52% rats**

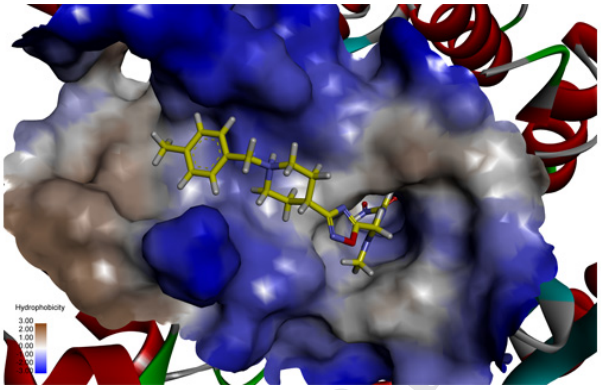

Discovery of 1,2,4-Oxadiazole-Containing Hydroxamic Acid Derivatives as Histone Deacetylase Inhibitors Potential Application in Cancer Therapy

Zhuang Yang[a], Mingsheng Shen[a], Minghai Tang[a], Wanhua Zhang[b], Xue Cui[a], Zihao Zhang[a], Heying Pei[a], Yong Li[a], Mengshi Hu[a], Peng Bai[a], and Lijuan Chen[*, a]

[a] State Key Laboratory of Biotherapy and Cancer Center, West China Hospital, Sichuan University and Collaborative Innovation Center of Biotherapy, Chengdu, 610041, China

[b] Department of Hematology and Research Laboratory of Hematology, West China Hospital of Sichuan University, Chengdu 610041, China

* **Corresponding author**. State Key Laboratory of Biotherapy and Cancer Center, West China Hospital, Sichuan University and Collaborative Innovation Center, Chengdu, Sichuan 610041, China.

Tel: +86-28-85164103; Fax: +86-28-85164060.

E-mail address: chenlijuan125@163.com.

ORCID

Chen, Lijuan: 0000-0002-8076-163X

Yang, Zhuang: 0000-0002-8915-9944

Abstract

In this study, a series of novel HDAC inhibitors, using 1,2,4-oxadiazole-containing as the cap group, were synthesized and evaluated in vitro. Compound **14b**, *N-hydroxy-2-(methyl((3-(1-(4-methylbenzyl)piperidin-4-yl)-1,2,4-oxadiazol-5-yl)methyl)amino)pyrimidine-5-carboxamide*, displayed the most potent histone deacetylase (HDAC) inhibition, especially against HDAC1, 2, and 3 with IC_{50} values of 1.8, 3.6 and 3.0 nM, respectively. In vitro antiproliferative studies confirmed that **14b** was more potent than SAHA, with IC_{50} values against 12 types of cancer cell lines ranging from 9.8 to 44.9 nM. The results of Western blot assays showed that compound **14b** can significantly up-regulate the acetylation of the biomarker his-H_3 and molecular docking analyses revealed the mode of action of compound **14b** against HDAC1. The results of flow-cytometry analysis suggested that compound **14b** induces cell cycle arrest at the G1 phase and has apoptotic effects. Further investigation of the activity of **14b** on the primary cells of three patients, showed IC_{50} values of 21.3, 61.1, and 77.4 nM. More importantly, an oral bioavailability of up to 53.52% was observed for **14b**. An in vivo pharmacodynamic evaluation demonstrated that compound **14b** can significantly inhibit tumor growth in a Daudi Burkitt's lymphoma xenograft model, with tumor inhibition rates of 53.8 and 46.1% observed at 20 and 10 mg/kg when administered p.o. and i.v., respectively. These results indicate that compound **14b** may be a suitable lead for further evaluation and development as an HDAC inhibitor and a potent anticancer agent.

Keywords: HDAC; 1,2,4-oxadiazole; antiproliferative; anticancer.

Introduction

Histone deacetylases (HDACs) are responsible for the deacetylation of lysine residues in histone or non-histone substrates,[1, 2] the epigenetic targeting of which has shown clinical benefits, especially for the treatment of cancer.[3] To date, 18 HDAC isoforms have been identified that are classified in four groups: classes I (HDAC1, 2, 3, and 8); II (HDAC4, 5, 6, 7, 9, and 10); III (SIRT1-7); and IV (HDAC11), depending on their sequence similarity, cellular localization, tissue expression patterns, and enzymatic mechanism.[4, 5] HDAC inhibitors can mediate cancer cell death by promoting reduced cell motility/migration, invasion, angiogenesis, proliferation, induction of apoptosis, and inhibition of DNA repair.[6-9] Currently, five HDAC inhibitors, vorinostat (SAHA),[10] romidepsin (FK-228),[11] belinostat (PXD-101),[12] panobinostat (LBH589),[13] and chidamide, have been approved for the treatment of cutaneous T-cell lymphoma (CTCL), peripheral T cell lymphoma (PTCL), or multiple myeloma (MM).[14] In addition, many inhibitors are currently in clinical trials for the treatment of hematological and/or solid tumors.[15] However, these drugs still have a number of problems. For instance, LBH589 has a "Highlights of prescribing information" boxed warning due to severe diarrhea occurring in 25% of LBH589-treated patients, with severe and fatal cardiac ischemic events, severe arrhythmias, and ECG changes also having occurred in patients receiving LBH589 treatment.[16] Due to decades of synthetic efforts, more than twenty candidates have entered clinical trials for a variety of disease treatments.[17] Although the use of unselective HDAC inhibitors outside of oncology is limited due to their side effects,[18-20] the benefit of isoform- or class-selective HDAC inhibitors in cancer therapy is still under debate. To date, there is no clear clinical evidence that isoform-selective HDAC inhibitors have sufficient efficacy while causing fewer adverse effects.[18-20] However, it is particularly important to develop a novel HDAC inhibitors with lower toxic side effects and better efficacy for cancer therapy.

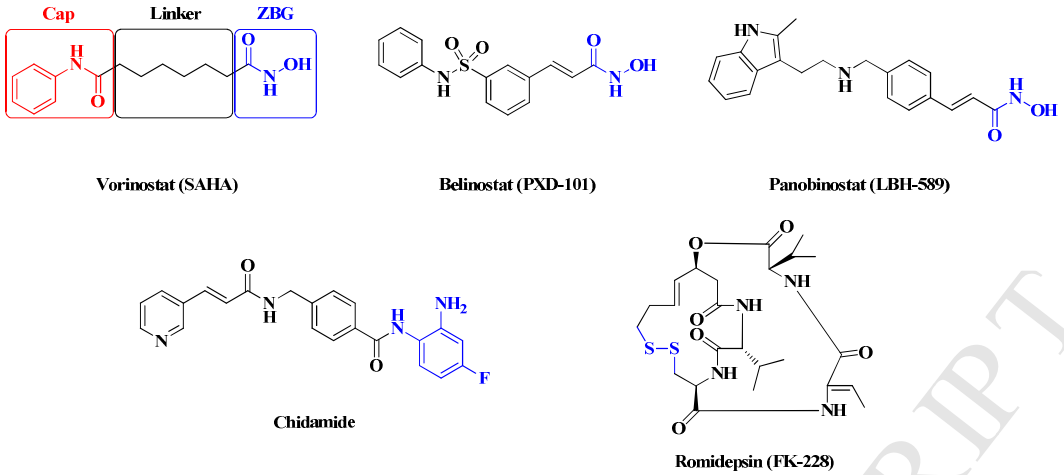

Figure 1. Licensed HDAC inhibitors

The pharmacophore models of most HDAC inhibitors always have three parts: a cap group used as a selective vector, a ZBG group to bind with the Zn^{2+} ion, and a linker region that traditionally allows the ZBG group stretch into the catalytic binding zone.[21-23] To date, modifications of the cap have been introduced that cause changes in HDAC potency and selectivity profiles.[24-29] In our previous study, we designed and synthesized a series of selective HDAC inhibitors by introducing different heterocyclic groups as the cap group, such as purine and quinoline groups.[30-32] Importantly, in 2014, Prof Antonello Mai et al reported a type of 1,3,4-oxadiazole-containing HDAC inhibitors with micromole antiproliferative activities against a panel of cancer cell lines.[33] Guided by the results of previous studies and available X-ray crystal structures[34, 35] or homology models generated by our lab[31], in this study, we describe the synthesis, biological evaluation, and modeling studies of a series of novel HDAC inhibitors that use 1,2,4-oxadiazole-containing derivatives as a cap group and exhibit nanomole antiproliferative activities and remarkable bioavailability as potent anticancer agents.

2. Results and Discussion

2.1 Chemistry

The synthetic route is presented in **Scheme 1-3**. *t*-Butyl

4-cyanopiperidine-1-carboxylate (**1**) was first reacted with hydroxylamine hydrochloride to generate compound **2**. Then, compound **2** and chloroacetyl chloride was reacted in the presence of triethylamine at room temperature, and without further purification, the crude compound was heated in 1,4-dioxane under reflux to obtain the intermediate compound **3**. The linker group was introduced by coupling compound **3** with methyl 4-hydroxycinnamate to obtain compound **4**, which was further de-protected of the Boc group to yield compound **5**. Subsequently, we used different R-Cl or R-Br compounds to react with compound **5** to obtain compounds **6**, which were directly converted to hydroxamic acid compounds **7** with NH_2OH.

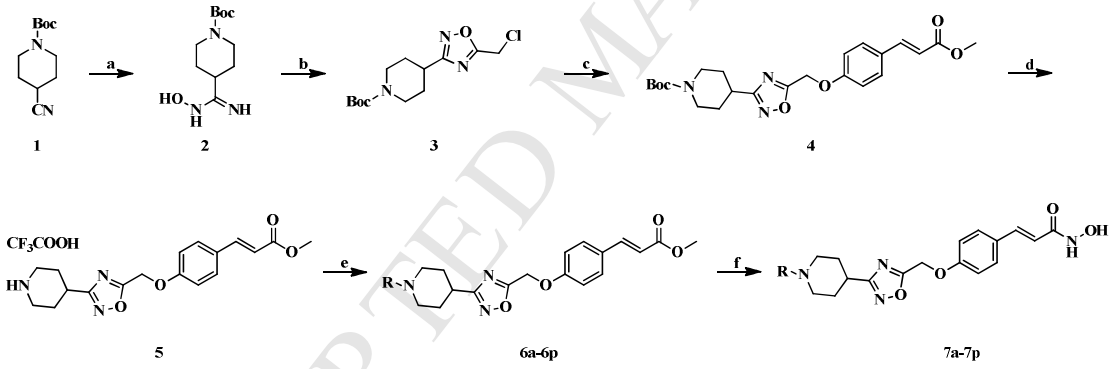

1 2 3 4 5 6a-6p 7a-7p

Scheme 1. Reagents and conditions: (a) $H_2NOH \cdot HCl$, $NaHCO_3$, $EtOH/H_2O$ (v/v, 5/1), reflux, overnight; (b) $ClCH_2COCl$, TEA, CH_2Cl_2, 0 ^oC to rt, 2 h; Dioxane, reflux, 2 h; (c) Methyl 4-hydroxycinnamate, $CsCO_3$, KI, MeCN, reflux, overnight; (d) CF_3COOH, CH_2Cl_2, rt, 4 h; (e) R-Cl or R-Br, K_2CO_3, KI, MeCN, rt, 4 h; (f) NH_2OH, NaOH, $MeOH/CH_2Cl_2$ (v/v, 2/1), rt, 2 h.

To evaluate the influence of linker groups on HDAC inhibition, we also synthesized a series of compounds using different commercially available compounds

that were reacted with the intermediate compound **3**. The resulting compounds **8** were further treated as previous described in **Scheme 1** to yield compounds **9** (**Scheme 2**).

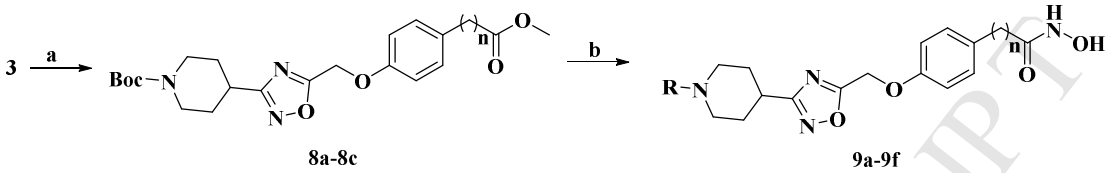

Scheme 2. Reagents and conditions: (a) $CsCO_3$, KI, MeCN, reflux, overnight; (b) i. CF_3COOH, CH_2Cl_2, rt, 4 h; ii. R-Cl or R-Br, K_2CO_3, KI, MeCN, rt, 4 h; iii NH_2OH, NaOH, MeOH/CH_2Cl_2 (v/v, 2/1), rt, 2 h.

For the pyrimidine structure used as the linker region, compounds **13a-13b** and **14a-14j** were synthesized to modify the SAR (**Scheme 2**). Compound **10** was synthesized by reacting compound **3** with methylamine, after which compound **10** was coupled with ethyl-2-chloropyrimidine-5-carboxylate and ethyl (*E*)-3-(2-chloropyrimidin-5-yl)acrylate to yield compounds **11** and **12**, respectively. Subsequently, compounds **11** and **12** were treated as described in **Scheme 1** to yield compounds **13a-13b** and **14a-14j**, respectively.

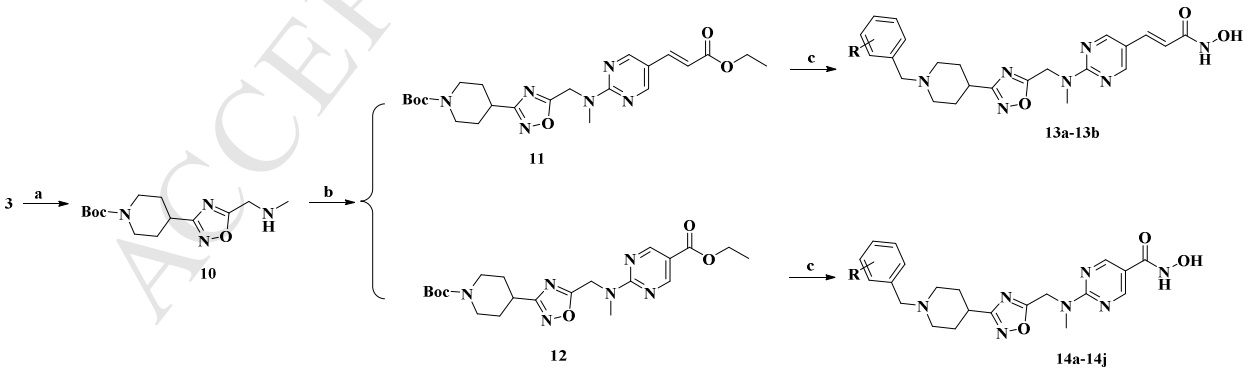

Scheme 3. Reagents and conditions: (a) Methylamine, EtOH, rt, 2 h; (b) DIPEA, MeOH, rt, 8 h; (c) i. CF_3COOH, CH_2Cl_2, rt, 4 h; ii. BnBr, K_2CO_3, KI, MeCN, rt, 4 h; iii NH_2OH, NaOH, MeOH/CH_2Cl_2 (v/v, 2/1), rt, 2 h.

2.2 Evaluation of the vitro activities evaluation of synthesized compounds

The synthesized compounds were initially evaluated for their inhibitory activities toward HDAC1 and HDAC6 at a concentration of 100 nM, the results of which are presented in **Tables 1**, **2** and **3**. As shown in **Table 1**, at 100 nM, compounds **7a-7p** all caused less than 50% inhibition of HDAC1, whereas more than 50% inhibition of HDAC6 was observed. Compound **7a**, which had an *n*-propyl chain introduced into the cap group, showed 40 and 69% inhibition of HDAC1 and HDAC6 at 100 nM respectively. However, the introduction of an unsaturated alkyl chain allyl group in compoudn **7b** caused a decrease in HDAC inhibition. Since the cap group promotes the ability of compounds to achieve selective inhibition of HDACs, a series substituted benzyl group were introduced. Compound **7c** displayed 71% inhibition of HDAC6 at 100 nM, whereas the inhibition of HDAC1 remained unchanged. When introducing substituted groups to the benzyl group, the inhibitory activities showed para- > meta- > ortho-position trend, such as compounds **7f**>**7e**>**7d,** in which a methyl groups were introduced, and **7i**>**7h**>**7g,** in which fluorine atoms were introduced. These results confirmed that para-position substitutions in these compouds could increase their inhibition of HDAC1 and HDAC6. When di-substituted benzyl groups were introduced, the ortho- and para- position-substituted compound **7j** was more effective than the meta- and para- position-substituted compound **7k**, with 35 and 17% inhibition of HDAC1 and 74 and 60% inhibition of HDAC6 observed, respectively. In contrast with compounds **7g** and **7i**, introducing the larger halogen chlorine (compound **7l**) and bromine atom (compound **7m)** caused significant decreases in HDAC inhibition. Compounds **7o** and **7p**, which had electron-withdrawing groups introduced, showed a reduction in HDAC1 and HDAC6 inhibition.

Table 1. Inhibition of HDAC1 and HDAC6 by compounds **7a-7p** (100 nM).[a]

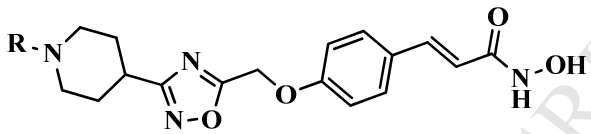

Compounds	R	% Inhibition		Compounds	R	% Inhibition	
		HDAC1	HDAC6			HDAC1	HDAC6
7a	Propyl	40	69	**7i**	4-F-Bn	38	75
7b	Allyl	34	66	**7j**	2,4-difluoro-Bn	35	74
7c	Bn	35	71	**7k**	3,4-difluoro-Bn	17	60
7d	2-Me-Bn	14	68	**7l**	2-Cl-Bn	8	59
7e	3-Me-Bn	25	73	**7m**	4-Br-Bn	6	58
7f	4-Me-Bn	32	76	**7n**	4-MeO-Bn	36	75
7g	2-F-Bn	31	68	**7o**	2-CN-Bn	36	65
7h	3-F-Bn	35	73	**7p**	2-NO_2-Bn	19	63

[a] Values are the averages of at least two independent experiments, SD < 10%.

To evaluate the influence of the linker group, the synthesized compounds **9a**-**9f** (100 nM) were also assessed for their ability to inhibit HDAC1 and HDAC6. As shown in **Table 2**, when the ethylene linkage was replaced by a saturated alkyl chain (compounds **9a** and **9b**) their inhibitory activities were significantly decreased, in contrast with the activities of compounds **7a** and **7b**, which have the same cap groups. The inhibitory activities of compounds **9c** and **9d**, in which benzyl groups were introduced to the cap groups, showed the same trends. The inhibitory activities of the compounds were significantly decreased, introducing benzyl groups to the cap groups was more favorable with respect to the inhibition of HDAC1 and HDAC6. The inhibitory activities of **9e** and **9f** were effectively increased with the decrease in carbon chain length. Taken together, these results suggest that the linker group is important for the inhibition of HDACs.

Table 2. Inhibition of HDAC1 and HDAC6 by compounds **9a-9f** (100 nM).[a]

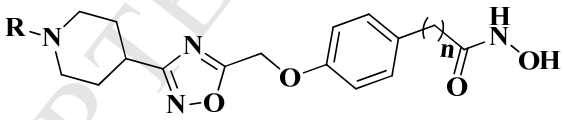

compounds	R	n	% inhibitory at 100 nM	
			HDAC1	HDAC6
9a	Propyl	2	5	13
9b	Allyl	2	4	15
9c	Bn	2	11	22
9d	4-Me-Bn	2	12	28
9e	Bn	1	18	35

9f	Bn	0	29	66

[a] Values are the averages of at least two independent experiments, SD < 10%.

Based on the SAR analysis, the synthesized compounds **13a**-**13b** and **14a**-**14j**, which had pyrimidine introduced into the linker region, were evaluated for their inhibitory activities toward HDAC1 and HDAC6 at concentrations at 100 nM and for their antiproliferative activities toward the Raji cell line, the results of which are presented in **Table 3**. In contrast with compounds **7c** and **7f,** which have vinyl groups in their linker regions, the inhibitory activities of compounds **13a** and **13b** toward HDAC1 were significantly improved, by 65% and 61% respectively. When the vinyl group was removed, compounds **14a** and **14b** showed increased inhibitory activities toward HDAC1 at 100 nM, both 96%, and the antiproliferative IC_{50} values toward B cell lymphoma Raji cell line were 27.6 and 12.1 nM, respectively. Based on this result, we further explored the effect of different substituted benzyl groups on the HDAC inhibitory activity. The inhibition of HDAC1 and HDAC6 as well as the antiproliferative activity of compound **14c** was reduced after shifting the methyl substitution to the meta position. Compounds **14d** and **14e** exhibit a similar SAR, with the F atom being the better substitution. A comparison of the activities of compounds **14f** and **14d** shows that the Cl substitution is better than F, but when F and Cl are simultaneously introduced into the molecule, the biological activity of **14j** was significantly reduced. When a 2,4-difluoro substitution was introduced, compound **14i** exhibited better antiproliferative activity, with an IC_{50} value 34.3 nM, although its activity against HDAC1 and HDAC6 decreased. When the electron-withdrawing groups CN (**14g**) or CF_3 (**14h**) were introduced in the para position, the HDAC inhibition and antiproliferative activities decreased. Based on the results of the SAR analysis, compound **14b** was selected as a seed compound for further research.

Table 3. Inhibition of HDAC1 and HDAC6 and antiproliferative activity toward the Raji cell line of compounds **13a**-**13b** and **14a**-**14j** (100 nM).[a]

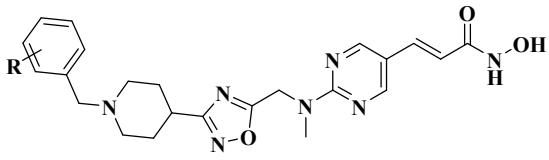

13a-13b

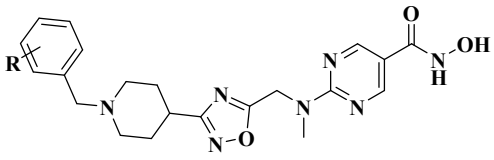

14a-14j

Compounds	R	% Inhibition		Raji
		HDAC1	HDAC6	IC_{50} (nM)
13a	H	65	55	547.3 ± 121.8
13b	4-Me	61	60	292.5 ± 79.4
14a	H	96	63	27.6 ± 3.8
14b	4-Me	96	71	12.1 ± 1.9
14c	3-Me	93	54	47.3 ± 3.1
14d	2-F	84	44	98.6 ± 8.6
14e	4-F	92	65	22.0 ± 3.2
14f	2-Cl	93	55	48.3 ± 5.7
14g	4-CN	68	38	116.6 ± 10.9
14h	4-CF_3	62	30	207 ± 32.3
14i	2,4-F	88	66	34.3 ± 2.8
14j	2-Cl-4-F	73	49	115.7 ± 15.7

[a] Values are the averages of at least two independent experiments, SD < 10%.

2.3 Compound 14b inhibitory activity toward HDAC1-11

Compound **14b** was further evaluated for its activity toward the other HDAC isoforms, the results of which are summarized in **Table 4**. Compound **14b** was effective toward class I HDAC1, 2, and 3, with IC_{50} values of 1.8, 3.6, and 3.0 nM respectively, which were more effective than SAHA. In contrast, the activity of compound **14b** toward class II and IV HDACs were relatively lower, especially toward HDAC11, with an observed IC_{50} value of more than 10 μM.

Table 4. HDAC inhibitory activity of compound **14b**

Isoform	IC_{50}[a] (nM)

		14b	SAHA
Class I	**HDAC1**	1.8 ± 0.2	20 ± 6
	HDAC2	3.6 ± 0.3	29 ± 4
	HDAC3	3.0 ± 0.8	33 ± 2
	HDAC8	260 ± 40	682 ± 87
Class IIa	**HDAC4**	473 ± 30	>10000
	HDAC5	540 ± 12	>10000
	HDAC7	392 ± 18	>10000
	HDAC9	441 ± 21	>10000
Class IIb	**HDAC6**	56 ± 1	27 ± 2
	HDAC10	102 ± 8	208 ± 19
Class IV	**HDAC11**	>10000	>10000

[a]: Compounds were tested in the 10-dose IC_{50} mode in duplicate with 3-fold serial dilutions starting at 10 μM. The IC_{50} values are the means of at least two experiments.

2.4 In vitro antiproliferative activity of 14b toward multiple tumor cell lines

To evaluate the antiproliferative activity of compound **14b**, the IC_{50} values toward 12 tumor cell lines were measured, including solid tumors (colon cancer HCT116, ovarian cancer A2780s, SKOV3, breast cancer MCF-7, MDA-MB-231, and liver cancer HepG2 cells) and hematological tumor (multiple myeloma ARD, MM1S, RPMI-8226, B cell lymphoma Raji, Jeko-1, and Ramos cells), by MTT, with SAHA used as the positive control. As presented in **Table 5**, compound **14b** possessed more potent inhibitory activity than SAHA. The IC_{50} values of compound **14b** ranged from 9.8 to 44.9 nM, whereas SAHA was weakly active toward the tumor cell lines, with IC_{50}s > 500 nM. Remarkably, compound **14b** was equally effective toward the solid and hematological tumor cell lines, whereas the traditional HDAC inhibitors such as SAHA are only effective toward hematological tumors. Those results confirmed that compound **14b** is a potent antitumor agent that could be used to treat solid tumors.

To determine the antiproliferative efficacy of **14b** toward primary cells, we

obtained PB blasts from three AML patients (Supplementary **Table S1**) and evaluated the antiproliferative activity of **14b** toward these cells. Compound **14b** effectively inhibited cell proliferation, with IC_{50} values of 21.2, 77.4, and 61.13 nM observed. These results prompted us to further study compound **14b**.

Table 5. The activity of compound **14b** against various human tumor cell lines and three primary AML cell lines.

Tumor type	Cell line	IC_{50} ± SD[a] (nM)	
		14b	**SAHA**
Colon	**HCT116**	16.0 ± 3.3	720.0 ± 45.3
Ovarian	**A2780s**	40.0 ± 19.5	5541.0 ± 833.0
	SKOV3	20.5 ± 5.4	1130.0 ± 236.5
Breast	**MCF-7**	14.4 ± 3.5	637.2 ± 56.4
	MDA-MB-231	25.6 ± 4.2	1710.0 ± 230.8
Liver	**HepG2**	13.0 ± 28	514.5 ± 93.1
Multiple myeloma	**ARD**	44.9 ± 1.8	630.1 ± 177.5
	MM1S	9.8 ± 1.1	590.3 ± 125.4
	RPMI-8226	15.6 ± 4.4	585.8 ± 116.5
B cell lymphoma	**Raji**	12.1 ± 1.9	867.4 ± 105.9
	Jeko-1	7.2 ± 1.7	638.6 ± 137.4
	Ramos	17.8 ± 0.5	514.6 ± 66.0
Primary AML cells	**Patient #1**	21.2 ± 3.4	ND
	Patient #1	77.4 ± 8.2	ND
	Patient #1	61.13 ± 13.7	ND

[a]: IC_{50} = concentration of the compound required to inhibit tumor cell proliferation by 50%. The data are expressed as the means ± SD from the dose-response curves of at least three independent experiments. ND: Not determined.

2.5 Upregulation of the acetylation of the histone H_3 and α-tubulin.

Upregulation of the acetylation of histone H_3 (substrate for HDAC 1, 2 and 3) and α-tubulin (substrate for HDAC6) are biomarkers of HDAC inhibition. To investigate the ability of compound **14b** in this context, western blot analysis of α-tubulin and histone H_3 acetylation in the MM1S cell line after 6 h of treatment with compound **14b** or SAHA at 40, 200, 1000, and 5000 nM was performed, the results of which are shown in **Figure 2**. Compound **14b** could induce the formation of Ac-H_3 and Ac-α-tubulin in a concentration-dependent manner, in agreement with the effects of SAHA. Notably, compound **14b** could significantly upregulate the acetylation of histone H_3 at 40 nM, whereas the acetylation level of α-tubulin could only be increased at high concentrations. This result confirmed the compound **14b** is an effective HDAC inhibitor.

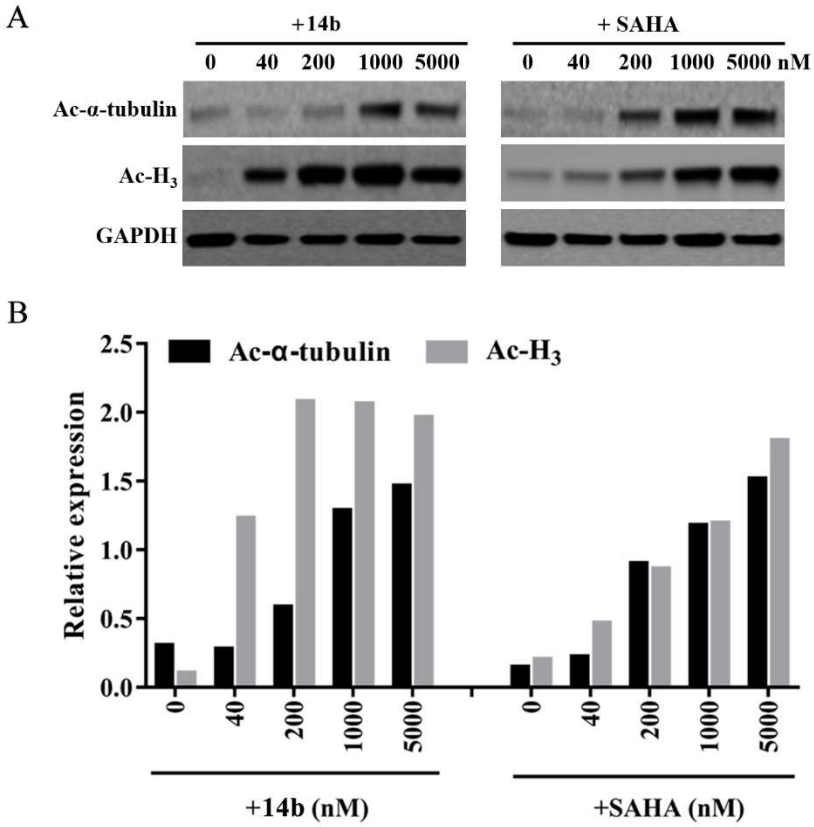

Figure 2. Western blot analysis of α-tubulin and histone H3 in the MM1S cell line after 6 h of treatment with compound **14b** or SAHA at 40, 200, 1000, and 5000 nM. GAPDH was used as a loading control.

2.6 Cell cycle and apoptotic induction assay

Previous studies have shown that the class I HDAC inhibitors promote the induction of apoptosis, cell differentiation, and cell growth arrest. We further evaluated compound **14b** for its ability effect on cell cycle arrest and the induction of apoptosis in B cell lymphoma Jeko-1 cells. The assays were performed at four different doses (0, 10, 100 and 1000 nM) for 24 and 48 h, the results of which are summarized in **Figure 3**. Consistent with previous reports, compound **14b** induced G1 cell cycle arrest in Jeko-1 cells after 24 h treatment in a dose-dependent manner (**Figure 3A** and **3B**). In addition, after 48 h of treatment, **14b** displayed a clear dose-dependent apoptotic effect in Jeko-1 cells, with the percentages of apoptosis cells increasing from 6.41 up to 73.1% (**Figure 3C** and **3D**). Thus, compound **14b** can block tumor cells in the G1-phase and induce tumor cell apoptosis in a dose-dependent manner.

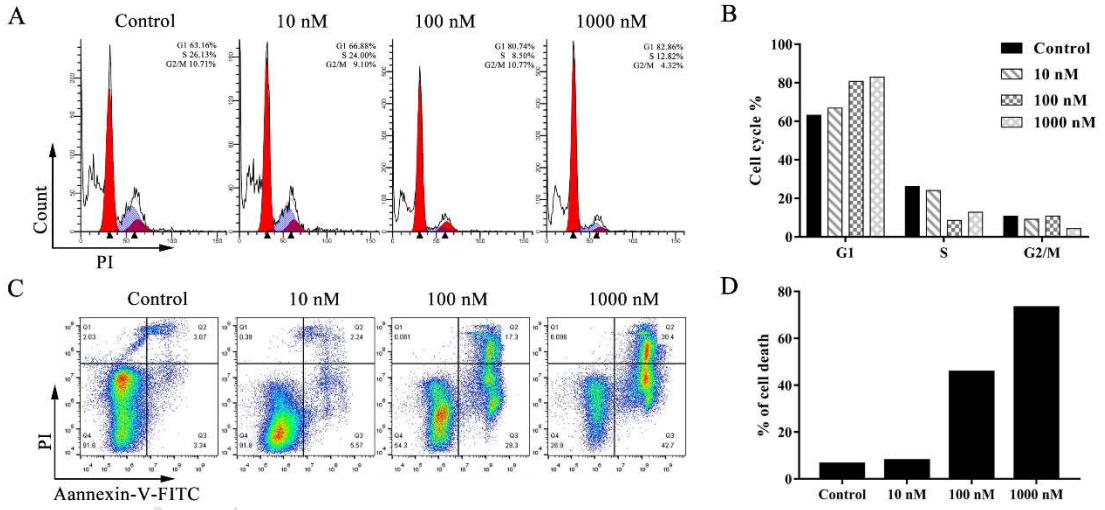

Figure 3. (A) and (B) Jeko-1 cells were cultured with **14b** (0, 10, 100, and 1000 nM) for 24 h and the cell cycle distribution of these cells was analyzed. (C) and (D) Jeko-1 cells were cultured with **14b** (0, 10, 100, and 1000 nM) for 48 h, and the cell apoptosis induction of these cells was analyzed.

2.7 Molecular docking

To identify potential interactions, compound **14b** was docked into a crystal

structure of HDAC1 (PDB code 4BKX) [36] using a previously reported method [30, 32, 37, 38]. In the predicted docking pose (shown in **Figure 4**), the hydroxyl group of the hydroxamic tail transferred a proton to a neighboring basic residue and formed a penta-coordination bond to a catalytic Zn^{2+} ion with the carbonyl group of the hydroxamic tail, that involved residues, His178, Asp264, and Asp176. Simultaneously, the NH of hydroxamic tail formed a hydrogen bond with the Gly149 residue. In the linker region, the pyrimidine and methyl groups were formed three weak hydrogen bonds with Gly149 and Asp99, with Asp99 also forming a pi-anion interaction with 1,2,4-oxadiazole. The piperidine ring allows the toluene ring to occupy a hydrophobic pocket on the surface of the HDAC1 protein. In addition to this hydrophobic interaction, the toluene formed a pi-donor hydrogen bonding interaction with His28, while there is no such interaction in the docking simulation result of HDAC6 with **14b** (Supplementary **Figure S1**). This result may explain the observed difference in activity of compound **14b** for HDAC1 over HDAC6. Therefore, these interactions appeared to enhance the binding affinity of **14b** for HDAC1.

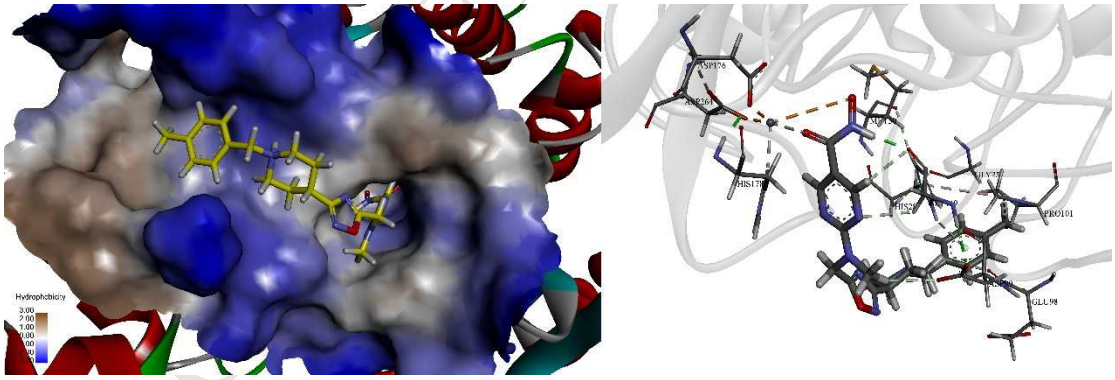

Figure 4. The binding models of **14b** in HDAC1 crystal structure (PDB code 4BKX).

2.8 Pharmacokinetic studies

HDAC inhibitors are well known to be limited by their low bioavailability, which limits the administration of these compounds. To investigate the bioavailability of compound **14b,** it was administered to SD rats at 5 mg/kg both intravenously (i.v.) and orally (p.o.), with blood samples subsequently analyzed for the concentration of

14b using an LC-MS/MS system. As shown in **Table 6**, the oral bioavailability of **14b** was excellent in rats, up to 53.52%, suggesting that **14b** is suitable both for i.v. and p.o. dosing as a potent anticancer agent.

Table 6. Pharmacokinetic parameters tested in vivo

Route	**14b**	
	i.v.	**p.o.**
N[a]	6	6
Dose (mg/kg)	5	5
Cl ($Lh^{-1}kg^{-1}$)[b]	11.87	22.31
V_{ss} (L/kg)[c]	6.33	29.13
AUC_{0-t} (μg/L*h)[d]	433.26	231.89
C_{max} (μg/L)[e]	954.91	240.96
$T_{1/2}$ (h)[f]	0.39	1.01
F (%)[g]	53.52	

[a]: Numbers of rats. [b]: Systemic clearance. [c]: Volume of distribution following intravenous dosing. [d]: Area under the curve following intravenous dosing, integrated drug concentration with respect to time and integrated drug concentration with respect to time following oral dosing. [e]: Maximum plasma concentration following intravenous dosing. [f]: Plasma half-life. [g]: Percent of bioavailability.

2.9 Antitumor activity in a Daudi xenograft model.

To determine the antitumor potency of compound **14b**, we established a Burkitt's lymphoma Daudi xenograft model. Compound **14b** was administrated three times over the cours of a week (10 mg/kg i.v. and 20 mg/kg p.o.). After the experiment was completed, the organ tissues and tumors of the experimental animals were collected, and the safety and effectiveness of compound **14b** were evaluated by H&E staining and immunohistochemistry analysis. As shown in **Figure 5A** and **5B**, **14b** promoted a remarkable reduction in tumor growth, with 46.1% (10 mg/kg, i.v.) and 53.8% (20

mg/kg, p.o.) TGI observed. It is worth noting that oral administration had a better effect than intravenous administration, which may be related to a higher bioavailability of compound **14b**. Immunohistochemical analysis showed that compared with the control group, the administration group exhibited significantly increased expression of Ac-H_4 in tumor tissues, inhibited the proliferation of tumor cells, and caused DNA damage of tumor cells, with the oral administration group being more effective than the intravenous group. In addition, all treated groups did not exhibit obvious abnormal behavior or significant toxic side effects, and H&E staining of organ tissues showed that compound **14b** did not cause organ damage in experimental animals (Supplementary **Figure S2**). These findings suggest that compound **14b** can be used as a potential oral anticancer drug.

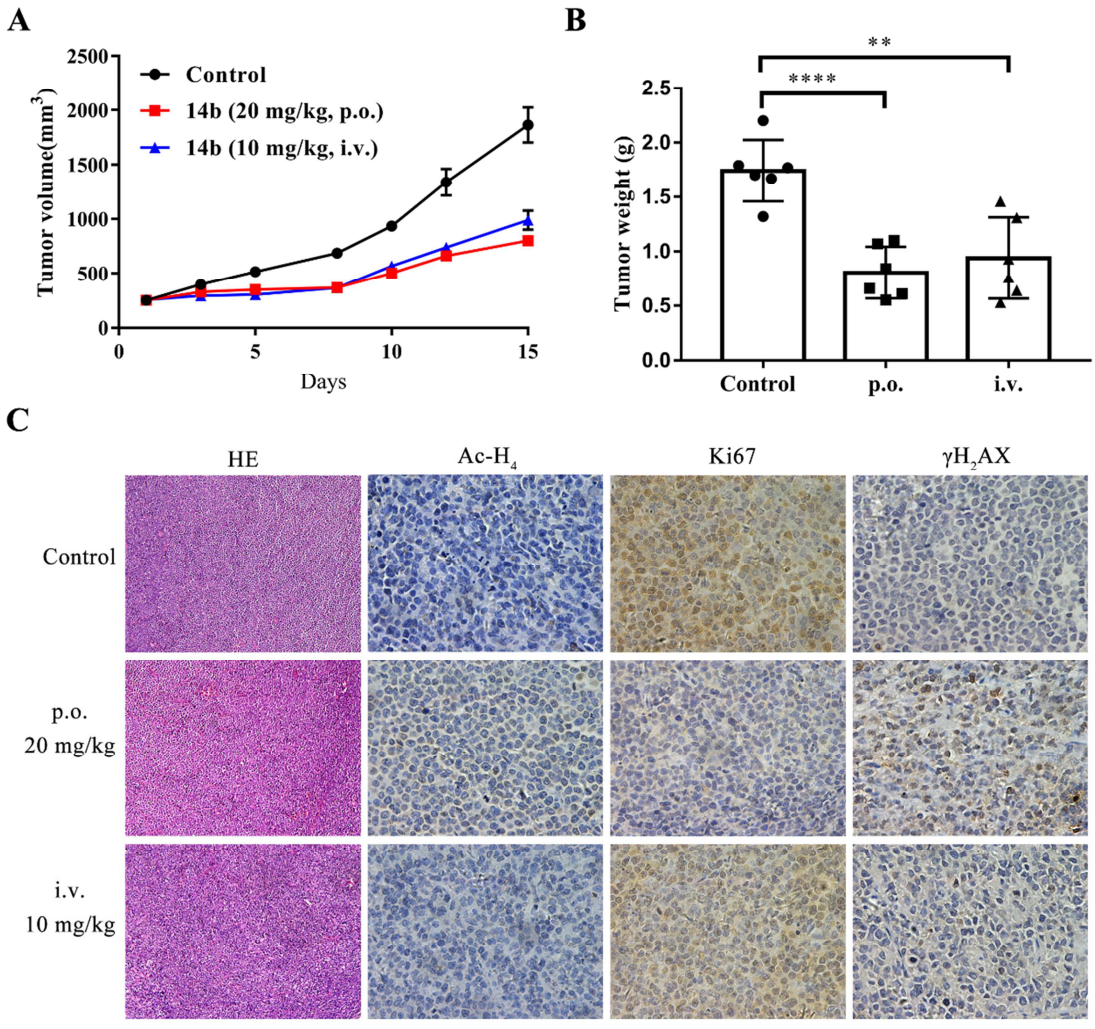

Figure 5. Antitumor effect of **14b** on the Daudi xenograft model. (A) Changes in tumor volume. (B) Tumor weight results. (c) H&E and immunohistochemistry results of tumor tissues.

3. Conclusion

In summary, in this study we developed a novel series of HDAC inhibitors with containing 1,2,4-oxadiazole as cap group and hydroxamic acid as ZBG group. The inhibitory activities of the synthesized compounds on the HDAC1 and 6 isoforms and a SAR analysis were performed. The most potent compound (**14b)** displayed optimal HDAC inhibitory activity, especially toward HDAC1, 2, and 3, with IC_{50} values 1.8, 3.6 and 3.0 nM, respectively, with the antiproliferative IC_{50} values ranging from 9.8 to 44.9 nM against 12 diverse cancer cell lines from both hematological and solid tumors. Importantly, **14b** also showed excellent antiproliferative activity against primary AML cells. The results of western blot analyses indicated that compound **14b** can increase the level of Ac-α-tubulin and Ac-H4 in a concentration-dependent manner, and molecular docking analysis showed the mode of action of compound **14b** with HDAC1. Further assays confirmed that compound **14b** could promote cell cycle arrest and induce apoptosis, while pharmacokinetic studies showed an up to 53.52% oral bioavailability of **14b**. In vivo pharmacodynamics experiments showed that compound **14b** achieved 46.1 and 53.8% inhibition at 10 and 20 mg/kg when i.v. and p.o. administered, respectively, with no significant side effects. These results show that compound **14b** represents a new scaffold to target HDAC for novel antitumor drug discovery.

4. Experimental section

4.1 Chemistry

All the chemical solvents and reagents, which were analytically pure without further purification, were commercially available. TLC was performed on 0.20 mm Silica Gel 60 F_{254} plates (Qingdao Ocean Chemical Factory, Shandong, China). Hydrogen nuclear magnetic resonance (^{1}H NMR) and carbon nuclear magnetic

resonance (^{13}C NMR) spectra were recorded on a Bruker Avance 400 spectrometer (Bruke Company, Germany) or Varian spectrometer (Varian, Palo Alto, CA). Chemical shifts are given in ppm relative to tetramethylsilane (TMS) as an internal standard, where TMS = 0.00 ppm. Mass spectra (MS) were measured by Q-TOF Priemier mass spectrometer (Micro mass, Manchester, UK). Room temperature (rt) is within the range 20-25 ^{o}C.

4.1.1. t-Butyl-4-(*N*'-hydroxycarbamimidoyl)piperidine-1-carboxylate **(2)**

The *t*-butyl-4-cyanopiperidine-1-carboxylate **1** (2.0 g, 9.51 mmol) was dissolved in ethanol (25 mL) and hydroxylamine hydrochloride (0.91 g, 14.27 mmol), water (5 mL) and sodium bicarbonate (1.6 g, 19.02 mmol) were added. The reaction mixture was stirred 1 h at ambient temperature and then heated overnight at reflux. After cooling to room temperature, the EtOH was removed in vacuo, and the aqueous layer was extracted with EtOAc (3 × 60 mL). The organic fractions were combined, washed with water (3 × 80 mL), then brine, and dried (Na_2SO_4). Removal of the sovent in vacuo afforded *t*-butyl-4-(*N*'-hydroxycarbamimidoyl)piperidine-1-carboxylate **2**. White solid, yield: 81.3%. ^{1}H NMR (400 MHz, DMSO-d_6) δ: 8.79 (s, 1H), 5.31 (s, 2H), 4.01–3.87 (m, 2H), 2.80–2.58 (m, 2H), 2.14 (tt, *J* = 11.7, 3.5 Hz, 1H), 1.72–1.62 (m, 2H), 1.49–1.40 (m, 2H), 1.39 (s, 9H). MS (ESI), m/z: 244.2 $[M + H]^+$.

4.1.2. t-Butyl-4-(5-(chloromethyl)-1,2,4-oxadiazol-3-yl)piperidine-1-carboxylate **(3)**

To a solution of the compound **2** (1.5 g, 6.17 mmol) in dichloromethane (25 mL) was added triethylamine (1.7 mL, 12.33 mmol) and the mixture was cooled to 0 °C. Chloroacetyl chloride (0.69 mL, 9.25 mmol) was slowly added dropwise over 5 min. The reaction was stirred at 0 °C for 10 min and then at room temperature for 2 h. The solvent was removed under vacuum and then the 1,4-dioxane solution was added and heated to reflux for 2 h. After completion of the reaction, the solvent was extracted with EtOAc, washed with water and brine, and dried with anhydrous Na_2SO_4. Then the solvent was removed under reduced pressure. The product was purified by Flash Chromatography eluting with 1/5 EtOAc/PE (petroleum ether) to give the title

compound **3**. Light yellow solid, yield: 79.2%. ^{1}H NMR (400 MHz, DMSO-d_6) δ: 5.08 (s, 2H), 3.99–3.88 (m, 2H), 3.06 (tt, *J* = 11.3, 3.8 Hz, 1H), 2.99–2.85 (m, 2H), 1.97–1.87 (m, 2H), 1.61–1.46 (m, 2H), 1.40 (s, 9H). MS (ESI), m/z: 302.2 $[M + H]^+$.

4.1.3.

t-Butyl-4-(5-((4-(3-methoxy-3-oxoprop-1-en-1-yl)phenoxy)methyl)-1,2,4-oxadiazol-3-yl)piperidine-1-carboxylate **(4)**

Preparation of the compound **3** (1 g, 3.31 mmol), methyl 4-hydroxycinnamate (0.65 g, 3.65 mmol), caesium carbonate (1.62 g, 4.97 mmol) and potassium iodide (54.8 mg, 0.3 mmol) were dissolved in acetonitrile (20 mL) and heated overnight at reflux. Reaction mixture was cooled and the solvent removed under vacuum. Extracted with EtOAc, washed with solution of sodium carbonate (Na_2CO_3) and brine, and dried with anhydrous Na_2SO_4. Then the solvent was removed under reduced pressure to provide the title compound **4**. White solid, yield: 90.2%. ^{1}H NMR (400 MHz, $CDCl_3$) δ: 7.64 (d, *J* = 16.0 Hz, 1H), 7.50 (d, *J* = 8.7 Hz, 2H), 7.00 (d, *J* = 8.8 Hz, 2H), 6.34 (d, *J* = 16.0 Hz, 1H), 5.29 (s, 2H), 4.21–4.06 (m, 2H), 3.80 (s, 3H), 3.04–2.96 (m, 1H), 2.96–2.87 (m, 2H), 2.06–1.95 (m, 2H), 1.84–1.71 (m, 2H), 1.47 (s, 9H). MS (ESI), m/z: 444.4 $[M + H]^+$.

4.1.4.

Methyl-3-(4-((3-(piperidin-4-yl)-1,2,4-oxadiazol-5-yl)methoxy)phenyl)acrylate-2,2,2-trifluoroacetate **(5)**

To a solution of intermediate **4** (1.25 g, 6.3 mmol) dissolved in dichloromethane (10 mL) was added TFA (2.34 mL) and the solution stirred at room temperature for 4 h. After completion of the reaction, the solvent removed under vacuum afforded an oily liquid which was added to a diethyl ether solution to precipitate a white solid. The white solid formed was collected by filtration and dried under vacuum to give the title compound **5.** White solid, yield: 95.1%.^{1}H NMR (400 MHz, DMSO-d_6) δ: 8.62 (s, 1H), 8.36 (s, 1H), 7.72 (d, *J* = 8.8 Hz, 2H), 7.63 (d, *J* = 16.0 Hz, 1H), 7.09 (d, *J* = 8.8 Hz, 2H), 6.54 (d, *J* = 16.0 Hz, 1H), 5.58 (s, 2H), 3.71 (s, 3H), 3.34–3.28 (m, 2H),

3.27–3.18 (m, 1H), 3.10–2.98 (m, 2H), 2.17–2.05 (m, 2H), 1.91–1.77 (m, 2H). MS (ESI), m/z: 344.2 $[M + H]^+$.

4.1.5. General procedure for synthesis of compounds **6a-p**

To a solution of the compound **5** (2.27 mmol) in acetonitrile (10 mL) was added potassium carbonate (4.53 mmol) and potassium iodide (0.2 mmol). Halide (2.49 mmol) was then added to the reaction mixture. The reaction mixture was stirred at room temperature for 4 h. The solvent removed under vacuum, extracted with EtOAc, the organic layers were combined, washed with water and brine, dried with $MgSO_4$, and concentrated in vacuo. Flash chromatography (5% EtOAc/petroleum ether to 30% EtOAc/petroleum ether) afforded the title compound **6a-p**.

4.1.5.1.

Methyl-3-(4-((3-(1-propylpiperidin-4-yl)-1,2,4-oxadiazol-5-yl)methoxy)phenyl)acrylate (**6a**). Pale yellow solid, yield: 83%. ^{1}H NMR (400 MHz, $CDCl_3$) δ: 7.64 (d, *J* = 16.0 Hz, 1H), 7.49 (d, *J* = 8.7 Hz, 2H), 7.00 (d, *J* = 8.8 Hz, 2H), 6.34 (d, *J* = 16.0 Hz, 1H), 5.28 (s, 2H), 3.80 (s, 3H), 3.05–2.96 (m, 2H), 2.89–2.78 (m, 1H), 2.43–2.31 (m, 2H), 2.19–1.87 (m, 6H), 1.62–1.50 (m, 2H), 0.91 (t, *J* = 7.3 Hz, 3H).

4.1.5.2.

Methyl-3-(4-((3-(1-allylpiperidin-4-yl)-1,2,4-oxadiazol-5-yl)methoxy)phenyl)acrylate (**6b**). White solid, yield: 87%. ^{1}H NMR (400 MHz, $CDCl_3$) δ: 7.64 (d, *J* = 16.0 Hz, 1H), 7.49 (d, *J* = 8.8 Hz, 2H), 7.00 (d, *J* = 8.8 Hz, 2H), 6.34 (d, *J* = 16.0 Hz, 1H), 5.96–5.83 (m, 1H), 5.28 (s, 2H), 5.25–5.15 (m, 2H), 3.80 (s, 3H), 3.10–3.03 (m, 2H), 3.02–2.95 (m, 2H), 2.90–2.79 (m, 1H), 2.25–2.03 (m, 4H), 2.00–1.88 (m, 2H).

4.1.5.3.

Methyl-3-(4-((3-(1-benzylpiperidin-4-yl)-1,2,4-oxadiazol-5-yl)methoxy)phenyl)acrylate (**6c**). White solid, yield: 88%. 1H NMR (400 MHz, DMSO-d_6) δ: 7.71 (d, *J* = 8.8 Hz, 2H), 7.63 (d, *J* = 16.0 Hz, 1H), 7.35–7.28 (m, 4H), 7.27–7.21 (m, 1H), 7.09 (d, *J*

= 8.8 Hz, 2H), 6.54 (d, *J* = 16.0 Hz, 1H), 5.55 (s, 2H), 3.71 (s, 3H), 3.48 (s, 2H), 2.87–2.75 (m, 3H), 2.14–2.03 (m, 2H), 1.97–1.87 (m, 2H), 1.78–1.61 (m, 2H). MS (ESI), m/z: 434.19 $[M + H]^+$.

4.1.5.4.

Methyl-3-(4-((3-(1-(2-methylbenzyl)piperidin-4-yl)-1,2,4-oxadiazol-5-yl)methoxy)phenyl)acrylate (**6d**). White solid, yield: 88%. ^{1}H NMR (400 MHz, $CDCl_3$) δ: 7.64 (d, *J* = 16.0 Hz, 1H), 7.49 (d, *J* = 8.8 Hz, 2H), 7.30–7.26 (m, 1H), 7.23–7.10 (m, 3H), 6.99 (d, *J* = 8.8 Hz, 2H), 6.33 (d, *J* = 16.0 Hz, 1H), 5.28 (s, 2H), 3.80 (s, 3H), 3.47 (s, 2H), 2.97–2.90 (m, 2H), 2.88–2.78 (m, 1H), 2.36 (s, 3H), 2.18–2.09 (m, 2H), 2.03–1.95 (m, 2H), 1.94–1.81 (m, 2H).

4.1.5.5.

Methyl-3-(4-((3-(1-(3-methylbenzyl)piperidin-4-yl)-1,2,4-oxadiazol-5-yl)methoxy)phenyl)acrylate (**6e**). White solid, yield: 81%. ^{1}H NMR (400 MHz, $CDCl_3$) δ: 7.64 (d, *J* = 16.0 Hz, 1H), 7.49 (d, *J* = 8.6 Hz, 2H), 7.21 (t, *J* = 7.4 Hz, 1H), 7.16 (s, 1H), 7.12 (d, *J* = 7.5 Hz, 1H), 7.07 (d, *J* = 7.3 Hz, 1H), 6.99 (d, *J* = 8.6 Hz, 2H), 6.33 (d, *J* = 16.0 Hz, 1H), 5.28 (s, 2H), 3.80 (s, 3H), 3.51 (s, 2H), 3.01–2.90 (m, 2H), 2.88–2.76 (m, 1H), 2.35 (s, 3H), 2.20–2.07 (m, 2H), 2.03–1.87 (m, 4H).

4.1.5.6.

Methyl-3-(4-((3-(1-(4-methylbenzyl)piperidin-4-yl)-1,2,4-oxadiazol-5-yl)methoxy)phenyl)acrylate (**6f**). White solid, yield: 85%. ^{1}H NMR (400 MHz, $CDCl_3$) δ: 7.64 (d, *J* = 16.0 Hz, 1H), 7.49 (d, *J* = 8.7 Hz, 2H), 7.21 (d, *J* = 7.8 Hz, 2H), 7.13 (d, *J* = 7.7 Hz, 2H), 6.99 (d, *J* = 8.6 Hz, 2H), 6.33 (d, *J* = 16.0 Hz, 1H), 5.27 (s, 2H), 3.80 (s, 3H), 3.49 (s, 2H), 2.98–2.89 (m, *J* = 11.4 Hz, 2H), 2.87–2.75 (m, 1H), 2.34 (s, 3H), 2.16–2.06 (m, 2H), 2.03–1.96 (m, 2H), 1.96–1.84 (m, 2H).

4.1.5.7.

Methyl-3-(4-((3-(1-(2-fluorobenzyl)piperidin-4-yl)-1,2,4-oxadiazol-5-yl)methoxy)phe

nyl)acrylate (**6g**). White solid, yield: 76%. ^{1}H NMR (400 MHz, $CDCl_3$) δ: 7.64 (d, *J* = 16.0 Hz, 1H), 7.49 (d, *J* = 8.8 Hz, 2H), 7.43–7.37 (m, 1H), 7.26–7.20 (m, 1H), 7.13–7.08 (m, 1H), 7.04 (d, *J* = 8.8 Hz, 1H), 6.99 (d, *J* = 8.8 Hz, 2H), 6.33 (d, *J* = 16.0 Hz, 1H), 5.28 (s, 2H), 3.80 (s, 3H), 3.61 (s, 2H), 3.01–2.92 (m, 2H), 2.86–2.77 (m, 1H), 2.23–2.14 (m, 2H), 2.04–1.98 (m, 2H), 1.97–1.88 (m, 2H).

4.1.5.8.

Methyl-3-(4-((3-(1-(3-fluorobenzyl)piperidin-4-yl)-1,2,4-oxadiazol-5-yl)methoxy)phenyl)acrylate (**6h**). White solid, yield: 80%. ^{1}H NMR (400 MHz, $CDCl_3$) δ: 7.64 (d, *J* = 16.0 Hz, 1H), 7.49 (d, *J* = 8.7 Hz, 2H), 7.32–7.27 (m, 1H), 7.14–7.07 (m, 2H), 7.00 (d, J = 8.8 Hz, 2H), 6.98–6.90 (m, 1H), 6.33 (d, J = 16.0 Hz, 1H), 5.28 (s, 2H), 3.80 (s, 3H), 3.54 (s, 2H), 2.99–2.79 (m, 3H), 2.27–1.84 (m, 6H).

4.1.5.9.

Methyl-3-(4-((3-(1-(4-fluorobenzyl)piperidin-4-yl)-1,2,4-oxadiazol-5-yl)methoxy)phenyl)acrylate (**6i**). White solid, yield: 82%. ^{1}H NMR (400 MHz, $CDCl_3$) δ: 7.64 (d, *J* = 16.0 Hz, 1H), 7.49 (d, *J* = 8.7 Hz, 2H), 7.32–7.26 (m, 2H), 7.03–6.95 (m, 4H), 6.33 (d, *J* = 16.0 Hz, 1H), 5.28 (s, 2H), 3.80 (s, 3H), 3.48 (s, 2H), 2.95–2.88 (m, 2H), 2.87–2.77 (m, 1H), 2.15–2.07 (m, 2H), 2.04–1.97 (m, 2H), 1.95–1.85 (m, 2H).

4.1.5.10

Methyl-3-(4-((3-(1-(2,4-difluorobenzyl)piperidin-4-yl)-1,2,4-oxadiazol-5-yl)methoxy)phenyl)acrylate (**6j**). White solid, yield: 86%. ^{1}H NMR (400 MHz, $CDCl_3$) δ: 7.64 (d, *J* = 16.0 Hz, 1H), 7.49 (d, *J* = 8.8 Hz, 2H), 7.37 (dd, *J* = 15.1, 8.4 Hz, 1H), 6.99 (d, *J* = 8.8 Hz, 2H), 6.89–6.75 (m, 2H), 6.33 (d, *J* = 16.0 Hz, 1H), 5.28 (s, 2H), 3.80 (s, 3H), 3.56 (s, 2H), 2.95–2.90 (m, 2H), 2.86–2.77 (m, 1H), 2.22–2.12 (m, 2H), 2.07–1.97 (m, 2H), 1.96–1.87 (m, 2H).

4.1.5.11.

Methyl-3-(4-((3-(1-(3,4-difluorobenzyl)piperidin-4-yl)-1,2,4-oxadiazol-5-yl)methoxy)

phenyl)acrylate (**6k**). White solid, yield: 89%. ^{1}H NMR (400 MHz, $CDCl_3$) δ: 7.64 (d, *J* = 16.0 Hz, 1H), 7.50 (d, *J* = 8.8 Hz, 2H), 7.23–7.16 (m, 1H), 7.13–7.05 (m, 1H), 7.05–7.02 (m, 1H), 7.00 (d, *J* = 8.8 Hz, 2H), 6.34 (d, *J* = 16.0 Hz, 1H), 5.29 (s, 2H), 3.80 (s, 3H), 3.46 (s, 2H), 2.94–2.87 (m, 2H), 2.87–2.79 (m, 1H), 2.18–2.08 (m, 2H), 2.06–1.98 (m, 2H), 1.96–1.84 (m, 2H).

4.1.5.12.

Methyl-3-(4-((3-(1-(2-chlorobenzyl)piperidin-4-yl)-1,2,4-oxadiazol-5-yl)methoxy)phenyl)acrylate (**6l**). Pale yellow solid, yield: 79%. ^{1}H NMR (400 MHz, $CDCl_3$) δ: 7.64 (d, *J* = 16.0 Hz, 1H), 7.50 (d, *J* = 8.7 Hz, 2H), 7.35 (d, *J* = 7.6 Hz, 1H), 7.25–7.14 (m, 3H), 7.00 (d, *J* = 8.7 Hz, 2H), 6.34 (d, *J* = 16.0 Hz, 1H), 5.29 (s, 2H), 3.80 (s, 3H), 3.66 (s, 2H), 3.14–2.94 (m, 2H), 2.91–2.76 (m, 1H), 2.38–2.18 (m, 2H), 2.13–1.84 (m, 4H).

4.1.5.13.

Methyl-3-(4-((3-(1-(4-bromobenzyl)piperidin-4-yl)-1,2,4-oxadiazol-5-yl)methoxy)phenyl)acrylate (**6m**). Yellow solid, yield: 81%. ^{1}H NMR (400 MHz, $CDCl_3$) δ: 7.64 (d, *J* = 16.0 Hz, 1H), 7.49 (d, *J* = 8.6 Hz, 2H), 7.44 (d, *J* = 8.1 Hz, 2H), 7.21 (d, *J* = 8.1 Hz, 2H), 7.00 (d, *J* = 8.5 Hz, 2H), 6.33 (d, *J* = 16.0 Hz, 1H), 5.28 (s, 2H), 3.80 (s, 3H), 3.48 (s, 2H), 2.94–2.88 (m, 2H), 2.87–2.78 (m, 1H), 2.18–2.07 (m, 2H), 2.05–1.97 (m, 2H), 1.96–1.83 (m, 2H).

4.1.5.14.

Methyl-3-(4-((3-(1-(4-methoxybenzyl)piperidin-4-yl)-1,2,4-oxadiazol-5-yl)methoxy)phenyl)acrylate (**6n**). White solid, yield: 86%. ^{1}H NMR (400 MHz, $CDCl_3$) δ: 7.64 (d, *J* = 16.0 Hz, 1H), 7.49 (d, *J* = 8.7 Hz, 2H), 7.30–7.22 (m, 2H), 6.99 (d, *J* = 8.7 Hz, 2H), 6.86 (d, *J* = 8.5 Hz, 2H), 6.33 (d, *J* = 16.0 Hz, 1H), 5.28 (s, 2H), 3.80 (s, 3H), 3.80 (s, 3H), 3.52 (s, 2H), 3.02–2.92 (m, 2H), 2.89–2.78 (m, 1H), 2.24–1.88 (m, 6H).

4.1.5.15.

Methyl-3-(4-((3-(1-(2-cyanobenzyl)piperidin-4-yl)-1,2,4-oxadiazol-5-yl)methoxy)phenyl)acrylate (**6r**). Pale yellow solid, yield: 75%. ^{1}H NMR (400 MHz, $CDCl_3$) δ: 7.66 (d, *J* = 4.5 Hz, 1H), 7.63 (d, *J* = 3.5 Hz, 1H), 7.61–7.53 (m, 2H), 7.49 (d, *J* = 8.7 Hz, 2H), 7.35 (t, *J* = 7.4 Hz, 1H), 7.00 (d, *J* = 8.7 Hz, 2H), 6.33 (d, *J* = 16.0 Hz, 1H), 5.28 (s, 2H), 3.80 (s, 3H), 3.73 (s, 2H), 2.99–2.91 (m, 2H), 2.90–2.81 (m, 1H), 2.32–2.21 (m, 2H), 2.06–1.99 (m, 2H), 1.98–1.87 (m, 2H).

4.1.5.16.

Methyl-3-(4-((3-(1-(2-nitrobenzyl)piperidin-4-yl)-1,2,4-oxadiazol-5-yl)methoxy)phenyl)acrylate (**6p**). Yellow solid, yield: 71%. ^{1}H NMR (400 MHz, $CDCl_3$) δ: 7.83 (d, *J* = 7.7 Hz, 1H), 7.68–7.61 (m, 2H), 7.58–7.52 (m, 1H), 7.50 (d, *J* = 8.7 Hz, 2H), 7.42–7.36 (m, 1H), 7.00 (d, *J* = 8.7 Hz, 2H), 6.34 (d, *J* = 16.0 Hz, 1H), 5.28 (s, 2H), 3.86–3.76 (m, 5H), 2.91–2.78 (m, 3H), 2.27–2.14 (m, 2H), 2.03–1.95 (m, 2H), 1.94–1.82 (m, 2H).

4.1.6. General procedure for synthesis of compounds **7a-p**

The ester intermediate (1 mmol) was dissolved in dichloromethane and methanol (1:2, 9 mL). The resulting solution was cooled to 0 ^{o}C, and then hydroxylamine (50 wt% in water, 30 mmol) and sodium hydroxide (2 mmol) were added. At the temperature, the reaction was stirred for 2 h. The solvent was then removed under reduced pressure, and the obtained solid was dissolved in water, which was adjusted to pH = 7–8 by acetic acid to precipitate a white solid. The white solid formed was collected by filtration to afford the crude **7a-p** and purified by flash chromatograph.

4.1.6.1.

N-Hydroxy-3-(4-((3-(1-propylpiperidin-4-yl)-1,2,4-oxadiazol-5-yl)methoxy)phenyl)acrylamide (**7a**). White powder, yield: 62%, m.p.: 133-135 ^{o}C. ^{1}H NMR (400 MHz, DMSO-d_6) δ: 7.58–7.49 (m, 2H), 7.41 (d, *J* = 15.8 Hz, 1H), 7.08 (d, *J* = 8.7 Hz, 2H), 6.34 (d, *J* = 15.8 Hz, 1H), 5.29 (s, 2H), 3.10–3.00 (m, 1H), 2.88–2.79 (m, 2H), 2.23 (m, 2H), 2.08–1.99 (m, 4H), 1.79–1.64 (m, 2H), 1.49–1.36 (m, 2H), 0.84 (t, *J* = 7.4

Hz, 3H). ^{13}C NMR (101 MHz, DMSO-d_6) δ: 183.08, 175.18, 166.80, 159.02, 129.50, 128.83, 115.65, 61.26, 60.41, 52.95, 52.62, 34.16, 29.96, 29.54, 20.09, 20.05, 12.31. MS (ESI), m/z: 387.2 $[M + H]^+$.

4.1.6.2.

3-(4-((3-(1-Allylpiperidin-4-yl)-1,2,4-oxadiazol-5-yl)methoxy)phenyl)-*N*-hydroxyacrylamide (**7b**). Pale yellow powder, yield: 66%, m.p.: 127-129 °C. ^{1}H NMR (400 MHz, DMSO-d_6) δ: 7.58–7.49 (m, 2H), 7.41 (d, *J* = 15.8 Hz, 1H), 7.08 (d, *J* = 8.4 Hz, 2H), 6.35 (dd, *J* = 15.8, 3.2 Hz, 1H), 5.89–5.75 (m, 1H), 5.30 (s, 2H), 5.22–2.06 (m, 2H), 3.11–3.00 (m,1H), 2.95 (d, *J* = 6.4 Hz, 2H), 2.88–2.78 (m, 2H), 2.13–1.89 (m,4H), 1.80–1.61 (m, 2H). ^{13}C NMR (101 MHz, DMSO-d_6) δ: 183.03, 175.20, 173.46, 166.81, 163.44, 136.08, 129.51, 117.90, 115.65, 61.49, 61.49, 61.25, 52.72, 52.38, 33.98, 33.65, 29.87, 29.45. MS (ESI), m/z: 385.1 $[M + H]^+$.

4.1.6.3.

3-(4-((3-(1-Benzylpiperidin-4-yl)-1,2,4-oxadiazol-5-yl)methoxy)phenyl)-*N*-hydroxyacrylamide (**7c**). White powder, yield: 71%, m.p.: 83-84 °C. ^{1}H NMR (400 MHz, DMSO-d_6) δ: 10.68 (s, 1H), 8.99 (s, 1H),7.53 (d, *J* = 8.3 Hz, 2H), 7.40 (d, *J* = 16.1 Hz, 1H), 7.36–7.28 (m, 4H), 7.27–7.22 (m, 1H), 7.07 (d, *J* = 8.7 Hz, 2H), 6.34 (d, *J* = 15.8 Hz, 1H), 5.52 (s, 2H), 3.48 (s, 2H), 2.88–2.73 (m, 3H), 2.13–2.03 (m, 2H), 1.97–1.85 (m, 2H), 1.78–1.61 (m, 2H). ^{13}C NMR (101 MHz, DMSO-d_6) δ: 175.20, 173.46, 166.81, 158.63, 138.89, 129.54, 129.23, 128.63, 127.34, 115.63, 62.76, 61.24, 52.76, 33.64, 29.91. MS (ESI), m/z: 435.16 $[M + H]^+$.

4.1.6.4.

N-Hydroxy-3-(4-((3-(1-(2-methylbenzyl)piperidin-4-yl)-1,2,4-oxadiazol-5-yl)methoxy)phenyl)acrylamide (**7d**). White powder, yield: 72%, m.p.: 154-156 °C. ^{1}H NMR (400 MHz, DMSO-d_6) δ: 7.51 (d, *J* = 6.9 Hz, 2H), 7.36 (d, *J* = 14.9 Hz, 1H), 7.22 (d, *J* = 5.8 Hz, 1H), 7.18–7.14 (m, 2H), 7.07 (d, *J* = 8.1 Hz, 3H), 6.33 (d, *J* = 15.7 Hz, 1H), 5.29 (s, 2H), 3.43 (s, 2H), 3.15–3.04 (m, 1H), 2.87–2.75 (m, 2H), 2.32 (s, 3H),

2.18–2.10 (m, 2H), 2.05–1.97 (m, 2H), 1.78–1.68 (m, 2H). ^{13}C NMR (101 MHz, DMSO-d_6) δ: 182.64, 166.42, 137.15, 136.46, 130.16, 129.61, 126.99, 125.47, 115.24, 94.85, 60.36, 52.21, 33.65, 29.18, 18.88. MS (ESI), m/z: 449.2 $[M + H]^+$.

4.1.6.5.

N-Hydroxy-3-(4-((3-(1-(3-methylbenzyl)piperidin-4-yl)-1,2,4-oxadiazol-5-yl)methoxy)phenyl)acrylamide (**7e**). White powder, yield: 68%, m.p.: 96-98 °C. ^{1}H NMR (400 MHz, DMSO-d_6) δ: 7.51 (d, *J* = 8.2 Hz, 2H), 7.37 (d, *J* = 15.6 Hz, 1H), 7.20 (t, *J* = 7.5 Hz, 1H), 7.11 (s, 1H), 7.10–7.03 (m, 4H), 6.34 (d, *J* = 15.7 Hz, 1H), 5.29 (s, 2H), 3.43 (s, 2H), 3.13–3.01 (m, 1H), 2.86–2.77 (m, 2H), 2.29 (s, 3H), 2.15–2.06 (m, 2H), 2.05–1.97 (m, 2H), 1.77–1.67 (m, 2H). ^{13}C NMR (101 MHz, DMSO-d_6) δ: 183.04, 166.82, 138.64, 137.67, 129.91, 129.41, 128.52, 128.02, 126.39, 115.63, 62.68, 61.25, 52.44, 33.98, 29.48, 21.48. MS (ESI), m/z: 449.3 $[M + H]^+$.

4.1.6.6.

N-Hydroxy-3-(4-((3-(1-(4-methylbenzyl)piperidin-4-yl)-1,2,4-oxadiazol-5-yl)methoxy)phenyl)acrylamide (**7f**). White powder, yield: 68%, m.p.: 135-137 °C. ^{1}H NMR (400 MHz, DMSO-d_6) δ: 7.47: (d, J = 8.6 Hz, 2H), 7.20 (d, *J* = 14.2 Hz, 1H), 7.18 (d, *J* = 7.8 Hz, 2H), 7.12 (d, *J* = 7.8 Hz, 2H), 7.03 (d, *J* = 8.6 Hz, 2H), 6.31 (d, *J* = 15.8 Hz, 1H), 5.27 (s, 2H), 3.43 (s, 2H), 3.12–2.99 (m,1H), 2.86–2.72 (m, 2H), 2.28 (s, 3H), 2.14–2.05 (m, 2H), 2.04–1.97(m, 2H), 1.80–1.65 (m, 2H). ^{13}C NMR (101 MHz, DMSO-d_6) δ: 183.02, 166.86, 158.34, 136.39, 135.59, 129.27, 129.21, 128.92, 115.55, 62.40, 61.24, 52.35, 34.01, 29.49, 21.16. MS (ESI), m/z: 449.4 $[M + H]^+$.

4.1.6.7.

3-(4-((3-(1-(2-Fluorobenzyl)piperidin-4-yl)-1,2,4-oxadiazol-5-yl)methoxy)phenyl)-*N*-hydroxyacrylamide (**7g**). White powder, yield: 65%, m.p.: 92-94 °C. ^{1}H NMR (400 MHz, DMSO-d_6) δ: 7.51 (d, *J* = 8.3 Hz, 2H), 7.40 (d, *J* = 8.7Hz, 1H), 7.36–7.28 (m, 2H), 7.21–7.15 (m, 2H), 7.07 (d, *J* = 8.5 Hz, 2H), 6.33 (d, *J* = 15.8 Hz, 1H), 5.29 (s, 2H), 3.55 (s, 2H), 3.12–3.01 (m, 1H), 2.88–2.75 (m, 2H), 2.19–2.12 (m, 2H), 2.06–

1.98 (m, 2H), 2.06–1.98 (m, 2H). ^{13}C NMR (101 MHz, DMSO-d_6) δ: 182.98, 166.82, 132.07, 129.58, 124.68, 115.73, 115.63, 115.50, 61.25, 55.11, 52.23, 33.85, 29.45. MS (ESI), m/z: 453.2 $[M + H]^+$.

4.1.6.8.

3-(4-((3-(1-(3-Fluorobenzyl)piperidin-4-yl)-1,2,4-oxadiazol-5-yl)methoxy)phenyl)-*N*-hydroxyacrylamide (**7h**). White powder, yield: 77%, m.p.: 86-88 °C. ^{1}H NMR (400 MHz, $CDCl_3$) δ: 7.67 (d, *J* = 15.7 Hz, 1H), 7.51 (d, *J* = 5.1 Hz, 2H), 7.32–7.27 (m, 1H), 7.10 (t, *J* = 9.1 Hz, 2H), 7.04–6.93 (m, 3H), 6.36 (d, *J* = 15.6 Hz, 1H), 5.29 (s, 2H), 3.62 (s, 2H), 3.09–2.95 (m, 2H), 2.91–2.77 (m, 1H), 2.31–2.16 (m, 2H), 2.11–1.88 (m, 4H). ^{13}C NMR (101 MHz, DMSO-d_6) δ: 183.03, 166.82, 133.06, 129.48, 128.68, 115.72, 115.53, 115.31, 61.25, 55.11, 52.24, 33.89, 29.46. MS (ESI), m/z: 453.3 $[M + H]^+$.

4.1.6.9.

3-(4-((3-(1-(4-Fluorobenzyl)piperidin-4-yl)-1,2,4-oxadiazol-5-yl)methoxy)phenyl)-*N*-hydroxyacrylamide (**7i**). White powder, yield: 76%, m.p.: 91-92 °C. ^{1}H NMR (400 MHz, DMSO-d_6) δ: 7.52 (d, *J* = 8.3 Hz, 2H), 7.39 (d, *J* = 14.2 Hz, 1H), 7.33 (dd, *J* = 8.5, 5.8 Hz, 2H), 7.14 (t, *J* = 8.9 Hz, 2H), 7.07 (d, *J* = 8.6 Hz, 2H), 6.34 (d, *J* = 15.8 Hz, 1H), 5.29 (s, 2H), 3.47 (s, 2H), 3.17–3.01 (m, 1H), 2.83–2.75 (m, 2H), 2.15–2.07 (m, 2H), 2.06–1.98 (m, 2H), 1.80–1.69 (m, 2H). ^{13}C NMR (101 MHz, DMSO-d_6) δ: 183.01, 166.82, 134.91, 131.11, 131.03, 129.42, 115.64, 115.45, 115.24, 61.67, 61.25, 52.29, 33.95, 29.46. MS (ESI), m/z: 453.2 $[M + H]^+$.

4.1.6.10.

3-(4-((3-(1-(2,4-Difluorobenzyl)piperidin-4-yl)-1,2,4-oxadiazol-5-yl)methoxy)phenyl)-N-hydroxyacrylamide (**7j**). White powder, yield: 65%, m.p.: 100-102 °C. ^{1}H NMR (400 MHz, DMSO-d_6) δ: 7.52 (d, *J* = 8.5 Hz, 2H), 7.49–7.42 (m, 1H), 7.40 (d, *J* = 15.9 Hz, 1H), 7.23–7.16 (m, 1H), 7.11–7.03 (m, 3H), 6.33 (d, *J* = 15.8 Hz, 1H), 5.29 (s, 2H), 3.52 (s, 2H), 3.13–3.02 (m, 1H), 2.87–2.77 (m, 2H), 2.19–2.10 (m, 2H), 2.06–

1.98 (m, 2H), 1.79–1.65 (m, 2H). ^{13}C NMR (101 MHz, DMSO-d_6) δ: 182.96, 166.81, 129.48, 115.64, 111.79, 104.31, 61.25, 54.61, 52.10, 33.82, 29.85, 29.43. MS (ESI), m/z: 471.2 $[M + H]^+$.

4.1.6.11.

3-(4-((3-(1-(3,4-Difluorobenzyl)piperidin-4-yl)-1,2,4-oxadiazol-5-yl)methoxy)phenyl)-N-hydroxyacrylamide (**7k**). White powder, yield: 75%, m.p.: 103-105 °C. ^{1}H NMR (400 MHz, $CDCl_3$) δ: 7.70 (d, *J* = 15.9 Hz, 1H), 7.52 (d, *J* = 8.6 Hz, 2H), 7.24–7.16 (m, 1H), 7.13–7.07 (m, 1H), 7.07–7.03 (m, 1H), 7.01 (d, *J* = 8.6 Hz, 2H), 6.35 (d, *J* = 16.0 Hz, 1H), 5.30 (s, 2H), 3.51 (s, 2H), 2.98–2.91 (m, 2H), 2.90–2.79 (m, 2H), 2.24–2.11 (m, 2H), 2.09–2.00 (m, 2H), 2.00–1.86 (m, 2H). ^{13}C NMR (101 MHz, DMSO-d_6) δ: 183.02, 166.82, 129.47, 115.61, 111.80, 104.29, 61.34, 54.61, 52.23, 33.87, 29.45. MS (ESI), m/z: 471.4 $[M + H]^+$.

4.1.6.12.

3-(4-((3-(1-(2-Chlorobenzyl)piperidin-4-yl)-1,2,4-oxadiazol-5-yl)methoxy)phenyl)-*N*-hydroxyacrylamide (**7l**). Yellow powder, yield: 71%, m.p.: 136-138 °C. ^{1}H NMR (400 MHz, DMSO-d_6) δ: 7.52 (d, *J* = 8.9 Hz, 2H), 7.46 (d, *J* = 22.1 Hz, 1H), 7.43–7.25 (m, 4H), 7.08 (d, *J* = 8.4 Hz, 2H), 6.34 (d, *J* = 15.7 Hz, 1H), 5.30 (s, 2H), 3.58 (s, 2H), 3.16–3.06 (m, 1H), 2.88–2.80 (m, 2H), 2.28–2.18 (m, 2H), 2.08–1.99 (m, 2H), 1.83–1.72 (m, 2H). ^{13}C NMR (101 MHz, DMSO-d_6) δ: 182.99, 166.82, 136.18, 133.74, 131.26, 129.72, 129.46, 129.06, 127.52, 115.64, 61.26, 59.15, 52.52, 33.85, 29.50. MS (ESI), m/z: 469.7 $[M + H]^+$.

4.1.6.13.

3-(4-((3-(1-(4-Bromobenzyl)piperidin-4-yl)-1,2,4-oxadiazol-5-yl)methoxy)phenyl)-*N*-hydroxyacrylamide (**7m**). Yellow powder, yield: 78%, m.p.: 98-100 °C. ^{1}H NMR (400 MHz, DMSO-d_6) δ: 7.51 (d, *J* = 8.3 Hz, 4H), 7.36 (d, *J* = 15.7 Hz, 1H), 7.27 (d, *J* = 8.3 Hz, 2H), 7.07 (d, *J* = 8.5 Hz, 2H), 6.34 (d, *J* = 15.8 Hz, 1H), 5.29 (s, 2H), 3.46 (s, 2H), 3.14–3.03 (m, 1H), 2.84–2.73 (m,2H), 2.18–2.07 (m, 2H), 2.06–1.97 (m, 2H),

1.82–1.66 (m, 2H). ^{13}C NMR (101 MHz, DMSO-d_6) δ: 182.99, 166.82, 138.29, 131.53, 131.39, 129.38, 120.38, 115.63, 61.71, 61.24, 52.32, 33.90, 29.46. MS (ESI), m/z: 513.5 $[M + H]^+$.

4.1.6.14.

N-Hydroxy-3-(4-((3-(1-(4-methoxybenzyl)piperidin-4-yl)-1,2,4-oxadiazol-5-yl)methoxy)phenyl)acrylamide (**7n**). White powder, yield: 78%, m.p.: 89-91 °C. ^{1}H NMR (400 MHz, DMSO-d_6) δ: 7.52 (d, *J* = 8.5 Hz, 2H), 7.40 (d, *J* = 15.8 Hz, 1H), 7.20 (d, *J* = 8.5 Hz, 2H), 7.07 (d, *J* = 8.7 Hz, 2H), 6.88 (d, *J* = 8.6 Hz, 2H), 6.34 (d, *J* = 15.8 Hz, 1H), 5.29 (s, 2H), 3.73 (s, 3H), 3.41 (s, 2H), 3.11–3.02 (m, 1H), 2.85–2.74 (m, 2H), 2.13–2.04 (m, 2H), 2.03–1.97 (m, 2H), 1.79–1.67 (m, 2H). ^{13}C NMR (101 MHz, DMSO-d_6) δ: 183.04, 166.80, 158.73, 130.50, 129.50, 115.65, 114.01, 62.05, 61.25, 55.45, 52.27, 34.03, 29.48. MS (ESI), m/z: 465.3 $[M + H]^+$.

4.1.6.15.

3-(4-((3-(1-(2-Cyanobenzyl)piperidin-4-yl)-1,2,4-oxadiazol-5-yl)methoxy)phenyl)-*N*-hydroxyacrylamide (**7o**). Pale yellow powder, yield: 61%, m.p.: 98-100 °C. ^{1}H NMR (400 MHz, DMSO-d_6) δ: 7.82 (d, *J* = 7.7 Hz, 1H), 7.68 (td, *J* = 7.7, 1.0 Hz, 1H), 7.59 (d, *J* = 7.7 Hz, 1H), 7.53 (d, *J* = 8.6 Hz, 2H), 7.47 (t, *J* = 7.6 Hz, 1H), 7.40 (d, *J* = 15.6 Hz, 1H), 7.08 (d, *J* = 8.6 Hz, 2H), 6.34 (d, *J* = 15.8 Hz, 1H), 5.30 (s, 2H), 3.67 (s, 2H), 3.18–3.07 (m, 1H), 2.88–2.75 (m, 2H), 2.31–2.16 (m, 2H), 2.10–1.98 (m, 2H), 1.84–1.65 (m, 2H). ^{13}C NMR (101 MHz, DMSO-d_6) δ: 182.94, 166.81, 142.66, 133.50, 130.56, 129.50, 128.46, 118.17, 115.64, 112.53, 61.25, 60.34, 52.36, 33.76, 29.40. MS (ESI), m/z: 460.3 $[M + H]^+$.

4.1.6.16.

N-Hydroxy-3-(4-((3-(1-(2-nitrobenzyl)piperidin-4-yl)-1,2,4-oxadiazol-5-yl)methoxy)phenyl)acrylamide (**7p**). Yellow powder, yield: 66%, m.p.: 106-107 °C. ^{1}H NMR (400 MHz, DMSO-d_6) δ: 7.85 (d, *J* = 8.0 Hz, 1H), 7.70–7.61 (m, 2H), 7.59–7.48 (m, 3H), 7.33 (d, *J* = 15.7 Hz, 1H), 7.06 (d, *J* = 8.4 Hz, 2H), 6.36 (d, *J* = 15.6 Hz, 1H), 5.28 (s,

2H), 3.74 (s, 2H), 3.13–3.01 (m, 1H), 2.74–2.64 (m, 2H), 2.25–2.10 (m, 2H), 2.01–1.84 (m, 2H), 1.73–1.57 (m, 2H). ^{13}C NMR (101 MHz, DMSO-d_6) δ: 182.90, 175.27, 173.35, 166.83, 150.10, 133.43, 133.33, 133.07, 131.51, 129.26, 128.98, 128.94, 124.58, 115.60, 61.24, 58.83, 58.70, 52.79, 52.44, 33.70, 33.38, 29.85, 29.45. MS (ESI), m/z: 480.2 $[M + H]^+$.

4.1.7. General procedure for synthesis of compounds **8a-c**

The compounds **8a-c** were prepared analogously starting from compound **3** and the appropriate phenol following the procedure for intermediate **4**.

4.1.7.1.

t-Butyl-4-(5-((4-(3-methoxy-3-oxopropyl)phenoxy)methyl)-1,2,4-oxadiazol-3-yl)piperidine-1-carboxylate (**8a**). White solid, yield: 91%. ^{1}H NMR (400 MHz, $CDCl_3$) δ: 7.07 (d, *J* = 8.6 Hz, 2H), 6.84 (d, *J* = 8.6 Hz, 2H), 5.16 (s, 2H), 4.10–4.01 (m, 2H), 3.60 (s, 3H), 2.97–2.89 (m, 1H), 2.88–2.79 (m, 4H), 2.53 (t, *J* = 7.7 Hz, 2H), 1.97–1.89 (m, 2H), 1.77–1.65 (m, 2H), 1.40 (s, 9H). MS (ESI), m/z: 456.3 $[M + H]^+$.

4.1.7.2.

t-Butyl-4-(5-((4-(2-methoxy-2-oxoethyl)phenoxy)methyl)-1,2,4-oxadiazol-3-yl)piperidine-1-carboxylate (**8b**). White solid, yield: 85%. ^{1}H NMR (400 MHz, $CDCl_3$) δ: 7.22 (d, *J* = 6.5 Hz, 2H), 6.95 (d, *J* = 6.5 Hz, 2H), 5.24 (s, 2H), 4.18–4.05 (m, 2H), 3.69 (s, 3H), 3.58 (s, 2H), 3.04–2.96 (m, 1H), 2.95–2.86 (m, 2H), 2.05–1.96 (m, 2H), 1.84–1.70 (m, 2H), 1.47 (s, 9H). MS (ESI), m/z: 432.2 $[M + H]^+$.

4.1.7.3.

t-Butyl-4-(5-((4-(ethoxycarbonyl)phenoxy)methyl)-1,2,4-oxadiazol-3-yl)piperidine-1-carboxylate (**8c**). White solid, yield: 87%. ^{1}H NMR (400 MHz, $CDCl_3$) δ: 8.03 (d, *J* = 8.9 Hz, 2H), 7.01 (d, *J* = 8.9 Hz, 2H), 5.31 (s, 2H), 4.36 (q, *J* = 7.1 Hz, 2H), 4.18–4.06 (m, 2H), 3.05–2.96 (m, 1H), 2.96–2.87 (m, 2H), 2.04–1.97 (m, 2H), 1.82–1.71 (m, 2H), 1.47 (s, 9H), 1.38 (t, *J* = 7.1 Hz, 3H). MS (ESI), m/z: 454.3 $[M + Na]^+$.

4.1.8. General procedure for synthesis of compounds **9a-f**

The compounds **9a-f** were prepared as described for compound **7a**.

4.1.8.1.

N-Hydroxy-3-(4-((3-(1-propylpiperidin-4-yl)-1,2,4-oxadiazol-5-yl)methoxy)phenyl)propanamide (**9a**). White powder, yield: 66%. ^{1}H NMR (400 MHz, DMSO-d_6) δ: 10.34 (s, 1H), 8.69 (s, 1H), 7.13 (dd, *J* = 8.4, 4.9 Hz, 2H), 6.94 (d, *J* = 8.6 Hz, 2H), 5.19 (s, 2H), 3.13–2.96 (m, 1H), 2.89–2.79 (m, 2H), 2.75 (t, *J* = 7.5 Hz, 2H), 2.22 (dd, *J* = 13.8, 6.5 Hz, 4H), 2.09–1.85 (m, 4H), 1.80–1.60 (m, 2H), 1.50–1.37 (m, 2H), 0.85 (t, *J* = 7.4 Hz, 3H). ^{13}C NMR (101 MHz, DMSO-*d*6) δ 182.98, 175.47, 173.47, 168.72, 167.03, 156.45, 156.12, 134.87, 134.50, 129.81, 129.74, 115.10, 115.08, 61.26, 60.49, 60.40, 56.50, 52.96, 52.63, 34.53, 34.49, 34.17, 33.84, 30.42, 29.96, 29.55, 20.09, 20.05, 19.02, 12.31. MS (ESI), m/z: 390.6 $[M + H]^+$.

4.1.8.2.

3-(4-((3-(1-Allylpiperidin-4-yl)-1,2,4-oxadiazol-5-yl)methoxy)phenyl)-*N*-hydroxypropanamide (**9b**). White powder, yield: 78%. ^{1}H NMR (400 MHz, DMSO-d_6) δ: 10.35 (s, 1H), 8.70 (s, 1H), 7.22–7.06 (m, 2H), 6.94 (d, *J* = 8.6 Hz, 2H), 5.88–5.75 (m, 1H), 5.43 (s, 1H), 5.22–5.08 (m, 3H), 2.95 (d, *J* = 6.3 Hz, 2H), 2.89–2.78 (m, 3H), 2.75 (t, *J* = 7.7 Hz, 2H), 2.22 (t, *J* = 7.6 Hz, 2H), 2.12–1.89 (m, 4H), 1.79–1.62 (m, 2H). ^{13}C NMR (101 MHz, DMSO-d_6) δ 182.93, 175.49, 173.43, 168.72, 167.04, 156.44, 156.12, 136.20, 136.07, 134.88, 134.50, 129.82, 129.74, 117.88, 117.76, 115.10, 115.08, 61.58, 61.48, 61.26, 52.72, 52.39, 34.53, 34.49, 34.00, 33.67, 30.41, 29.87, 29.46. MS (ESI), m/z: 387.0 $[M + H]^+$.

4.1.8.3. 3-(4-((3-(1-Benzylpiperidin-4-yl)-1,2,4-oxadiazol-5-yl)methoxy)phenyl)-*N*-hydroxypropanamide (**9c**). White powder, yield: 82%. ^{1}H NMR (400 MHz, DMSO-d_6) δ: 7.33–7.29 (m, 4H), 7.27–7.22 (m, 1H), 7.16–7.11 (m, 2H), 6.94 (d, *J* = 8.6 Hz, 2H), 5.42 (s, 2H), 3.48 (s, 2H), 2.87–2.78 (m, 3H), 2.75 (t, *J* = 7.6 Hz, 2H), 2.22 (t, *J* = 7.7

Hz, 2H), 2.12–2.05 (m, 2H), 1.96–1.87 (m, 2H), 1.75–1.67 (m, 2H). ^{13}C NMR (101 MHz, DMSO-d_6) δ 182.93, 175.49, 175.43, 173.43, 168.62, 168.60, 167.03, 156.44, 156.11, 138.88, 138.72, 134.91, 134.54, 129.82, 129.74, 129.26, 129.23, 128.62, 127.37, 127.33, 115.09, 115.07, 62.77, 62.66, 61.26, 52.77, 52.42, 34.58, 34.54, 34.00, 33.67, 30.46, 29.90, 29.48, 24.94, 19.92. MS (ESI), m/z: 437.1 $[M + H]^+$.

4.1.8.4.

N-Hydroxy-3-(4-((3-(1-(4-methylbenzyl)piperidin-4-yl)-1,2,4-oxadiazol-5-yl)methoxy)phenyl)propanamide (**9d**). White powder, yield: 78%. ^{1}H NMR (400 MHz, DMSO-d_6) δ: 10.35 (s, 1H), 8.70 (s, 1H), 7.18 (d, *J* = 7.9 Hz, 2H), 7.15–7.10 (m, 4H), 6.94 (d, *J* = 8.6 Hz, 2H), 5.19 (s, 2H), 3.43 (s, 2H), 2.86–2.76 (m, 3H), 2.75 (t, *J* = 7.7 Hz, 2H), 2.28 (s, 3H), 2.22 (t, *J* = 7.6 Hz, 2H), 2.14–1.86 (m, 4H), 1.79–1.60 (m, 2H). ^{13}C NMR (101 MHz, DMSO-d_6) δ 182.95, 175.49, 173.44, 168.68, 167.03, 156.44, 156.12, 136.39, 136.34, 135.76, 135.60, 134.88, 134.50, 129.82, 129.74, 129.26, 129.23, 129.20, 115.10, 115.07, 62.51, 62.40, 61.26, 52.71, 52.36, 34.49, 34.02, 33.69, 30.42, 29.92, 29.50, 21.16. MS (ESI), m/z: 451.0 $[M + H]^+$.

4.1.8.5.

2-(4-((3-(1-Benzylpiperidin-4-yl)-1,2,4-oxadiazol-5-yl)methoxy)phenyl)-*N*-hydroxyacetamide (**9e**). White powder, yield: 77%. ^{1}H NMR (400 MHz, DMSO-d_6) δ: 10.47 (s, 1H), 8.83 (s, 1H), 7.35–7.28 (m, 4H), 7.27–7.22 (m, 1H), 7.18 (d, *J* = 8.5 Hz, 2H), 6.96 (d, *J* = 8.5 Hz, 2H), 5.21 (s, 2H), 3.48 (s, 2H), 3.20 (s, 2H), 3.12–3.02 (m, 1H), 2.86–2.77 (m, 2H), 2.16–2.06 (m, 2H), 2.06–1.98 (m, 2H), 1.80–1.64 (m, 2H). ^{13}C NMR (101 MHz, DMSO-d_6) δ 182.95, 175.45, 173.43, 167.60, 166.99, 156.81, 138.90, 138.75, 130.55, 130.47, 129.60, 129.25, 129.22, 128.63, 127.36, 127.33, 115.03, 115.00, 62.77, 62.66, 61.25, 52.78, 52.43, 38.92, 34.01, 29.92, 29.50. MS (ESI), m/z: 423.0 $[M + H]^+$.

4.1.8.6

4-((3-(1-Benzylpiperidin-4-yl)-1,2,4-oxadiazol-5-yl)methoxy)-*N*-hydroxybenzamide

(**9f**). White powder, yield: 75%. ^{1}H NMR (400 MHz, DMSO-d_6) δ: 11.08 (s, 1H), 8.95 (s, 1H), 7.73 (d, *J* = 8.8 Hz, 2H), 7.35–7.28 (m, 4H), 7.27–7.22 (m, 1H), 7.09 (d, *J* = 8.9 Hz, 2H), 5.31 (s, 2H), 3.48 (s, 2H), 3.13–3.03 (m, 1H), 2.89–2.73 (m, 2H), 2.16–2.07 (m, 2H), 2.06–1.98 (m, 2H), 1.81–1.66 (m, 2H). ^{13}C NMR (101 MHz, DMSO-d_6) δ 183.05, 175.11, 173.47, 166.75, 164.19, 160.21, 129.26, 129.23, 129.10, 128.64, 127.37, 126.40, 114.90, 62.65, 61.28, 52.41, 34.00, 29.91, 29.49. MS (ESI), m/z: 409.0 $[M + H]^+$.

4.1.9 *tert*-Butyl 4-(5-((methylamino)methyl)-1,2,4-oxadiazol-3-yl)piperidine-1-carboxylate (**10**). Compound **3** (0.6 g, 2 mmol) was dissolved in 30% methylamine (15 mL) and stirred for 2 h at room temperature. After completion of the reaction, the solvent was removed under reduced pressure. The resulting was dissolved in ethyl acetate, and washed with water. The organic phase was further removed under reduced pressure, and got the desired product **10**. ^{1}H NMR (400 MHz, DMSO-d_6) δ: 4.02 (s, 2H), 3.04–2.81 (m, 3H), 2.53 (s, 3H), 2.05–1.95 (m, 2H), 1.91–1.70 (m, 2H), 1.47 (s, 9H). MS (ESI), m/z: 297.2 $[M + H]^+$.

4.1.10 *tert*-Butyl (*E*)-4-(5-(((5-(3-ethoxy-3-oxoprop-1-en-1-yl)pyrimidin-2-yl)(methyl)amino)methyl)-1,2,4-oxadiazol-3-yl)piperidine-1-carboxylate (**11**). Compound **10** (0.3 g, 1 mmol) and methyl (*E*)-3-(2-chloropyrimidin-5-yl)acrylate (0.2 g, 1 mmol) were dissolved in MeOH (15 mL), DIPEA (2.5 mL, 1.5 mmol) was added into the solution. The reaction was stirred overnight at room temperature. Then the solvent was removed, the residue was dissolved in ethyl acetate and washed with water. The organic phase was further removed under reduced pressure, and got the desired product **11** (66% yield, yellow solid). ^{1}H NMR (400 MHz, $CDCl_3$) δ: 8.50 (s, 2H), 7.51 (d, *J* = 16.1 Hz, 1H), 6.33 (d, *J* = 16.1 Hz, 1H), 5.11 (s, 2H), 3.80 (s, 3H), 3.37 (s, 3H), 2.99–2.88 (m, 2H), 2.84–2.70 (m, 1H), 2.15–2.05 (m, 2H), 2.03–1.81 (m, 4H), 1.39 (s, 9H). MS (ESI), m/z: 481.0 $[M + Na]^+$.

4.1.11 Ethyl 2-(((3-(1-(tert-butoxycarbonyl)piperidin-4-yl)-1,2,4-oxadiazol-5-yl)methyl)(methyl)amino)pyrimidine-5-carboxylate (**12**). Compound **10** (0.3 g, 1 mmol) and methyl ethyl 2-chloropyrimidine-5-carboxylate (0.2 g, 1 mmol) were dissolved in MeOH (15 mL), DIPEA (2.5 mL, 1.5 mmol) was added into the solution. The reaction was stirred overnight at room temperature. Then the solvent was removed, the residue was dissolved in ethyl acetate and washed with water. The organic phase was further removed under reduced pressure, and got the desired product **12** (71% yield, white solid). ^{1}H NMR (400 MHz, DMSO-d_6) δ: 8.83 (m,2H), 5.20 (s, 2H), 4.27 (q, J = 7.1 Hz, 2H), 3.98–3.83 (m, 2H), 3.32 (s, 3H), 2.98 (tt, J = 11.2, 3.7 Hz, 1H), 2.92–2.81 (m, 2H), 1.93–1.85 (m, 2H), 1.54–1.41 (m, 2H), 1.39 (s, 9H), 1.29 (t, J = 7.1 Hz, 3H). MS (ESI), m/z: 469.7 $[M + Na]^+$.

4.1.12.1 (*E*)-3-(2-(((3-(1-Benzylpiperidin-4-yl)-1,2,4-oxadiazol-5-yl)methyl)(methyl)amino)pyrimidin-5-yl)-*N*-hydroxyacrylamide (**13a**). The compound **13a** was synthesized as **7a-7p**. Yellow solid. ^{1}H NMR (400 MHz, DMSO-d_6) δ: 8.63 (s, 2H), 7.35–7.27 (m, 5H), 7.27–7.21 (m,1H), 6.38 (d, J = 16.0 Hz, 1H), 5.15 (s, 2H), 3.47 (s, 2H), 3.30 (s, 3H), 2.84–2.78 (m, 2H), 2.77–2.71 (m, 1H), 2.10–2.02 (m, 2H), 1.91–1.84 (m, 2H), 1.70–1.59 (m, 2H). ^{13}C NMR (101 MHz, DMSO-d_6) δ 177.05, 173.31, 161.34, 138.85, 129.17, 128.59, 127.29, 118.66, 117.21, 70.20, 62.73, 52.74, 45.71, 36.44, 33.62, 29.87. m/z: 450.5 $[M + H]^+$.

4.1.12.2 (*E*)-*N*-hydroxy-3-(2-(methyl((3-(1-(4-methylbenzyl)piperidin-4-yl)-1,2,4-oxadiazol-5-yl)methyl)amino)pyrimidin-5-yl)acrylamide (**13b**). The compound **13b** was synthesized as **7a-7p**. Yellow solid. ^{1}H NMR (400 MHz, DMSO-d_6) δ: 8.61 (s, 2H), 7.31 (d, J = 15.9 Hz, 1H), 7.16 (d, J = 7.9 Hz, 2H), 7.11 (d, J = 7.9 Hz, 2H), 6.38 (d, J = 15.9 Hz, 1H), 5.14 (s, 2H), 3.41 (s, 2H), 3.29 (s, 3H), 2.82–2.76 (m, 2H), 2.76–2.69

(m, 1H), 2.27 (s, 3H), 2.08–1.97 (m, 2H), 1.92–1.82 (m, 2H), 1.69–1.56 (m, 2H). ^{13}C NMR (101 MHz, DMSO-d_6) δ 177.05, 173.37, 161.41, 157.51, 136.32, 135.76, 129.20, 129.18, 118.74, 117.28, 62.52, 52.72, 45.73, 36.45, 33.70, 29.92, 21.15. MS (ESI), m/z: 464.3 $[M + H]^+$.

4.1.13.1

2-(((3-(1-Benzylpiperidin-4-yl)-1,2,4-oxadiazol-5-yl)methyl)(methyl)amino)-*N*-hydroxypyrimidine-5-carboxamide (**14a**). The compound **14a** was synthesized as **7a**-**7p**. White solid. ^{1}H NMR (400 MHz, DMSO-d_6) δ: 11.10 (s, 1H), 9.04 (s, 1H), 8.69 (s, 2H), 7.35–7.21 (m, 5H), 5.16 (s, 2H), 3.47 (d, *J* = 3.9 Hz, 2H), 3.30–3.22 (m, 3H), 3.07–2.96 (m, 1H), 2.84–2.76 (m, 2H), 2.13–2.01 (m, 2H), 2.0– 1.84 (m, 2H), 1.77–1.57 (m, 2H). ^{13}C NMR (101 MHz, DMSO-d_6) δ: 182.31, 176.51, 172.98, 167.30,161.82, 138.50, 138.34, 128.85, 128.82, 128.23, 126.97, 126.93, 115.72, 62.37, 62.25, 52.39, 52.03, 45.33, 44.60, 36.08, 35.68, 33.60, 33.27, 29.51, 29.13. MS (ESI), m/z: 424.6 $[M + H]^+$.

4.1.13.2

N-hydroxy-2-(methyl((3-(1-(4-methylbenzyl)piperidin-4-yl)-1,2,4-oxadiazol-5-yl)methyl)amino)pyrimidine-5-carboxamide (**14b**). The compound **14b** was synthesized as **7a**-**7p**. White solid. ^{1}H NMR (400 MHz, DMSO-d_6) δ 11.11 (s, 1H), 9.05 (s, 1H), 8.69 (s, 2H), 7.19 (d, *J* = 7.7 Hz, 2H), 7.13 (d, *J* = 7.5 Hz, 2H), 5.16 (s, 2H), 3.47 (s, 2H), 3.29 (s, 3H), 2.80 (d, *J* = 25.3 Hz, 3H), 2.28 (s, 3H), 2.09 (s, 2H), 1.89 (d, *J* = 13.5 Hz, 3H), 1.66 (d, *J* = 13.2 Hz, 2H). ^{13}C NMR (101 MHz, DMSO-d_6) δ: 176.50, 172.98, 161.82, 135.93, 135.36, 128.82, 128.79, 115.73, 62.12, 52.33, 45.33, 36.08, 33.30, 29.52, 20.76. MS (ESI), m/z: 438.37 $[M + H]^+$.

4.1.13.3

N-hydroxy-2-(methyl((3-(1-(3-methylbenzyl)piperidin-4-yl)-1,2,4-oxadiazol-5-yl)methyl)amino)pyrimidine-5-carboxamide (**14c**). The compound **14c** was synthesized as **7a**-**7p**. White solid. ^{1}H NMR (400 MHz, DMSO-d_6) δ 11.09 (s, 1H), 9.03 (s, 1H),

8.68 (s, 2H), 7.19 (t, *J* = 7.5 Hz, 1H), 7.12–7.01 (m, 3H), 5.15 (s, 2H), 3.41 (s, 2H), 3.29 (s, 2H), 2.84–2.69 (m, 3H), 2.29 (s, 3H), 2.09–2.00 (m, 2H), 1.87 (d, *J* = 10.6 Hz, 2H), 1.64 (qd, *J* = 12.1, 3.7 Hz, 2H). ^{13}C NMR (101 MHz, DMSO-d_6) δ 182.70, 176.90, 173.38, 167.71, 162.18, 138.80, 137.63, 129.84, 128.49, 127.96, 126.36, 126.33, 116.27, 62.81, 52.82, 52.46, 45.71, 36.45, 33.69, 29.91, 29.52, 21.46. MS (ESI), m/z: 438.19 $[M + H]^+$.

4.1.13.4

2-(((3-(1-(2-fluorobenzyl)piperidin-4-yl)-1,2,4-oxadiazol-5-yl)methyl)(methyl)amino)-*N*-hydroxypyrimidine-5-carboxamide (**14d**). The compound **14d** was synthesized as **7a-7p**. White solid. ^{1}H NMR (400 MHz, DMSO-d_6) δ 11.09 (s, 1H), 9.03 (s, 1H), 8.68 (s, 2H), 7.40 (td, *J* = 7.7, 1.8 Hz, 1H), 7.34-7.27 (m, 1H), 7.21–7.11 (m, 2H), 5.15 (s, 2H), 3.53 (d, *J* = 5.0 Hz, 2H), 3.26 (d, *J* = 22.7 Hz, 3H), 2.86–2.79 (m, 2H), 2.79-2.69 (m, 1H), 2.12 (q, *J* = 11.6 Hz, 2H), 1.93 (dd, *J* = 39.4, 11.0 Hz, 2H), 1.76–1.57 (m, 2H). ^{13}C NMR (101 MHz, DMSO-d_6) δ 182.61, 176.90, 173.28, 167.66, 162.41, 162.14, 159.98, 132.02, 131.96, 131.91, 129.46, 129.38, 125.16, 125.02, 124.85, 124.62, 124.59, 116.13, 115.68, 115.65, 115.44, 55.14, 55.05, 52.56, 52.21, 45.69, 44.96, 36.44, 36.03, 33.82, 33.49, 29.83, 29.45. MS (ESI), m/z: 442.23 $[M + H]^+$.

4.1.13.5

2-(((3-(1-(4-fluorobenzyl)piperidin-4-yl)-1,2,4-oxadiazol-5-yl)methyl)(methyl)amino)-*N*-hydroxypyrimidine-5-carboxamide (**14e**). The compound **14e** was synthesized as **7a-7p**. White solid. ^{1}H NMR (400 MHz, DMSO-d_6) δ 11.10 (s, 1H), 9.04 (s, 1H), 8.69 (s, 2H), 7.32 (dd, *J* = 8.2, 5.9 Hz, 2H), 7.13 (td, *J* = 8.9, 2.1 Hz, 2H), 5.16 (s, 2H), 3.45 (d, *J* = 4.0 Hz, 2H), 3.26 (d, *J* = 22.5 Hz, 3H), 2.80-2.71 (m, 3H), 2.07 (q, *J* = 11.7 Hz, 2H), 1.92 (dd, *J* = 39.7, 11.4 Hz, 2H), 1.76–1.58 (m, 2H). ^{13}C NMR (101 MHz, DMSO-d_6) δ 182.68, 176.91, 173.36, 167.70, 162.22, 135.07, 131.09, 131.04, 130.96, 115.43, 115.22, 61.80, 61.68, 52.66, 52.31, 45.73, 36.47, 33.97, 33.64, 29.90, 29.51. MS (ESI), m/z: 442.11 $[M + H]^+$.

940

941 4.1.13.6

942 2-(((3-(1-(2-chlorobenzyl)piperidin-4-yl)-1,2,4-oxadiazol-5-yl)methyl)(methyl)amino

943)-N-hydroxypyrimidine-5-carboxamide (**14f**). The compound **14f** was synthesized as

944 **7a-7p**. White solid. ^{1}H NMR (400 MHz, DMSO-d_6) δ 10.97 (s, 1H), 9.04 (s, 1H),

945 8.68 (s, 2H), 7.49 (dd, *J* = 7.6, 1.6 Hz, 1H), 7.44-7.40 (m, 1H), 7.35-7.25 (m, 2H),

946 5.16 (s, 2H), 3.57 (d, *J* = 4.0 Hz, 2H), 3.27 (d, *J* = 22.5 Hz, 3H), 2.85-2.75 (m, 3H),

947 2.18 (q, *J* = 11.4 Hz, 2H), 1.94 (dd, *J* = 41.6, 9.2 Hz, 2H), 1.79–1.61 (m, 2H). ^{13}C

948 NMR (101 MHz, DMSO-d_6) δ 182.62, 176.91, 173.29, 167.67, 162.14, 136.24,

949 136.12, 133.68, 133.64, 131.19, 131.15, 129.66, 129.64, 129.00, 128.95, 127.47,

950 59.21, 59.12, 52.86, 52.52, 45.69, 44.96, 36.45, 36.04, 33.82, 33.50, 29.89, 29.50. MS

951 (ESI), m/z: 458.08 $[M + H]^+$.

952

953 4.1.13.7

954 2-(((3-(1-(4-cyanobenzyl)piperidin-4-yl)-1,2,4-oxadiazol-5-yl)methyl)(methyl)amino)

955 -*N*-hydroxypyrimidine-5-carboxamide (**14g**). The compound **14g** was synthesized as

956 **7a-7p**. White solid. ^{1}H NMR (400 MHz, DMSO-d_6) δ 11.10 (s, 1H), 9.04 (s, 1H),

957 8.68 (s, 1H), 7.61 (d, *J* = 6.9 Hz, 1H), 7.29 (d, *J* = 7.9 Hz, 1H), 5.15 (s, 2H), 3.48 (d, *J*

958 = 3.6 Hz, 2H), 3.26 (d, *J* = 22.4 Hz, 3H), 2.81-2.71 (m, 3H), 2.08 (q, *J* = 11.6 Hz, 2H),

959 1.93 (dd, *J* = 39.5, 11.8 Hz, 2H), 1.76-1.60 (m, 2H). ^{13}C NMR (101 MHz, DMSO-d_6)

960 δ 182.69, 176.91, 173.36, 167.70, 169.30, 162.20, 151.26, 139.71, 139.55, 132.55,

961 132.51, 128.95, 128.92, 127.90, 125.74, 116.20, 115.77, 62.41, 62.30, 52.79, 52.44,

962 45.73, 45.00, 36.47, 36.07, 33.98, 33.65, 29.91, 29.53. MS (ESI), m/z: 449.53 [M +

963 H]$^+$.

964

965 4.1.13.8

966 *N*-hydroxy-2-(methyl((3-(1-(4-(trifluoromethyl)benzyl)piperidin-4-yl)-1,2,4-oxadiazo

967 l-5-yl)methyl)amino)pyrimidine-5-carboxamide (**14h**). The compound **14h** was

968 synthesized as **7a-7p**. White solid. ^{1}H NMR (400 MHz, DMSO-d_6) δ 11.00 (s, 1H),

969 9.07 (s, 1H), 8.68 (s, 2H), 7.68 (d, *J* = 8.1 Hz, 2H), 7.54 (d, *J* = 8.0 Hz, 2H), 5.16 (s,

2H), 3.56 (s, 2H), 3.29 (s, 3H), 2.78 (td, *J* = 11.7, 6.4 Hz, 3H), 2.16–2.05 (m, 2H), 1.95–1.84 (m, 2H), 1.66 (qd, *J* = 12.4, 3.5 Hz, 2H). ^{13}C NMR (101 MHz, DMSO-d_6) δ 176.90, 173.28, 162.14, 161.96, 144.02, 129.68, 128.12, 127.80, 126.14, 125.47, 125.43, 125.39, 123.44, 116.11, 61.94, 52.75, 45.68, 36.42, 33.49, 29.84. MS (ESI), m/z: 492.36 $[M + H]^+$.

4.1.13.9

2-(((3-(1-(2,4-difluorobenzyl)piperidin-4-yl)-1,2,4-oxadiazol-5-yl)methyl)(methyl)amino)-*N*-hydroxypyrimidine-5-carboxamide (**14i**). The compound **14i** was synthesized as **7a**-**7p**. White solid. ^{1}H NMR (400 MHz, DMSO-d_6) δ 11.10 (s, 1H), 9.03 (s, 1H), 8.68 (s, 2H), 7.48–7.39 (m, 1H), 7.23–7.14 (m, 1H), 7.05 (td, *J* = 8.7, 2.1 Hz, 1H), 5.15 (s, 2H), 3.50 (s, 2H), 3.26 (d, *J* = 22.8 Hz, 3H), 2.76 (dd, *J* = 30.8, 11.4 Hz, 2H), 2.16–2.04 (m, 2H), 1.88 (d, *J* = 10.6 Hz, 2H), 1.70–1.54 (m, 2H). ^{13}C NMR (101 MHz, DMSO-d_6) δ 182.26, 176.90, 173.31, 167.70, 162.21, 160.69, 160.57, 159.88, 133.14, 121.62, 121.47, 116.16, 111.76, 111.56, 104.28, 104.02, 103.76, 54.69, 52.47, 52.12, 45.72, 36.46, 33.50, 29.85, 29.47. MS (ESI), m/z: 460.10 $[M + H]^+$.

4.1.13.10

2-(((3-(1-(2-chloro-4-fluorobenzyl)piperidin-4-yl)-1,2,4-oxadiazol-5-yl)methyl)(methyl)amino)-*N*-hydroxypyrimidine-5-carboxamide (**14j**). The compound **14j** was synthesized as **7a**-**7p**. White solid. ^{1}H NMR (400 MHz, DMSO-d_6) δ 10.97 (s, 1H), 9.16 (s, 1H), 8.68 (s, 2H), 7.52 (dd, *J* = 8.6, 6.5 Hz, 1H), 7.39 (dd, *J* = 8.9, 2.6 Hz, 1H), 7.20 (td, *J* = 8.5, 2.6 Hz, 1H), 5.14 (s, 2H), 3.53 (s, 2H), 3.28 (s, 3H), 2.86–2.73 (m, 3H), 2.21–2.12 (m, 2H), 1.88 (d, *J* = 10.8 Hz, 2H), 1.66 (qd, *J* = 12.7, 12.3, 3.6 Hz, 2H). ^{13}C NMR (101 MHz, DMSO-d_6) δ 182.58, 177.01, 173.26, 167.72, 162.49, 162.09, 161.95, 160.04, 134.32, 134.27, 132.66, 132.62, 132.59, 132.54, 132.51, 116.94, 116.68, 114.72, 114.51, 58.55, 58.45, 52.75, 52.41, 45.67, 44.93, 36.41, 36.00, 33.80, 33.47, 29.87, 29.48. MS (ESI), m/z: 476.27 $[M + H]^+$.

4.2 In vitro HDAC enzymatic assay

The HDACs inhibitory activity assay in vitro was conducted utilizing 7-amino-4-methylcoumarin (AMC) labeled Ac-peptide (Ac-peptide-AMC) substrates, performed by Chempartner Company (Shanghai, China). Briefly, upon deacetylation of the substrate, the release of AMC was promoted in the existence of trypsin. The compounds, diluted to the specified concentrations, were mixed with full-length recombinant HDAC enzymes (BPS Biosciences), trypsin, and Ac-peptide-AMC substrates, incubated at room temperature for 1 h. The fluorescence was measured with excitation at the wavelength of 355 nm and emission at the wavelength of 460 nm, using a multilabel plate reader. The inhibition rates of the test groups were calculated by comparison with the DMSO (vehicle) treat group.

4.3 AML patient samples

Primary cells of AML patients samples were obtained and approved via West China Hospital of Sichuan University (Chengdu, China) and the clinical information are summarized in supplementary Table S1.

4.4 MTT assay

A2780s, SKOV3, HCT116, MCF-7, MDA-MB-231 and HepG2 cells were cultured in DMEM (Gibco, Milano, Italy). MM1S, ARD, RPMI-8226, Jeko-1, Ramos and Raji cells were cultured in RPMI-1640 medium (Gibco, Milano, Italy). All of the above media contained 10% fetal bovine serum (FBS) (Invitrogen, Milano, Italy), 100 units/mL penicillin (Gibco, Milano, Italy), and 100 μg/mL streptomycin (Gibco, Milano, Italy). Cells were incubated at 37 °C in a humidified atmosphere of 5% CO_2. Cells in logarithmic phase were seeded into 96-well culture plates at densities of 3000-5000 cells per well and subsequently treated with various concentrations of compounds for 72 h in final volumes of 200 μL. Upon end point, 20 μL of MTT (5 mg/mL) was added to each well, and the cells were incubated for an additional 1-3 h. After carefully removal of the medium, the precipitates were dissolved in 150 μL of DMSO via mechanically shaking, and then absorbance values at a wavelength of 570 nm were taken on a spectrophotometer (Molecular Devices, Sunnyvale, USA). IC_{50}

values were calculated using percentage of growth versus untreated control.

4.5 Western blot assay

The cells were treated with the compounds at the indicated concentrations. After washing by PBS 2 times, the cells were resuspended in RIPA lysis buffer (Beyotime Co.). After 30 min of incubation on ice, the lysates were collected by centrifuging at 12000 g for 15 min at 4 °C. The protein concentration was measured. Equivalent samples (20 μg of protein) were subjected to 15% SDS-PAGE, and then the proteins were transferred onto activated PVDF membranes (Millipore, USA). After blocking by 5% non-fat milk for 1 h at room temperature, the membranes were incubated with the indicated primary antibodies at 4 ^{o}C and subsequently probed by the appropriate secondary antibodies conjugated to horseradish peroxidase for 1 h. Immunoreactive bands were visualized using enhanced chemiluminescence (Millipore, USA).

4.6 Pharmacokinetic assay

The animal protocol was approved by the Animal Care and Use Committee of Sichuan University in China (IACUC number: 20100318). A 1 mg/mL dosing solution was preparing by dissolving the appropriate amount of the compound in 3% ethanol and 1% tween80 in normal saline. SD rats, weighing 200-250 g each, were abtained from Beijing HFK Bioscience Co., Ltd. The tested compound was separately administered intravenously to a group of six rats per time point (5 mg/kg dose) by a bolus injection (5 mg/kg) to the tail vein or periorally. At time points 0 (prior to dosing), 5 min, 15 min, 30 min, 45 min, 1 h, 2 h, 4 h, 6 h, 8 h, 10 h, 12 h, and 24 h after dosing, a blood sample was collected from each animal via cardiac puncture and stored in ice (0-4 ^{o}C). Plasma was separated from the blood by centrifugation (4000 g for 15 min at 4 ^{o}C) and stored in a freezer at -80 ^{o}C. All samples were analyzed for the test compound by LC-MS/MS (Waters Acquity UPLC system; Waters Quattro Premier XE). Data were acquired via monitoring of multiple reactions. Plasma concentration data were analyzed by a standard noncompartmental method.

4.7 Animal Tumor Models and Treatment

To establish the Daudi xenograft model, Daudi cells (107 cells in 100 μL serum-free RPMI 1640) were injected subcutaneously into the right flanks of 5−6 week old female NOD/SCID mice. When the size of the formed xenografts reached 100−200 mm^3, the mice were randomly divided (six mice per group). The mice in the experimental group received i.v. (10 mg/kg, dissolved in 8% HP-β-CD) and p.o. (20 mg/kg, dissolved in 8% HP-β-CD) treatment, 1st, 3rd, and 5th days per week. Tumor burden was measured every 2 days by a caliper. Tumor volume (TV) was calculated using the following formula: TV = length × width2 × 0.5. At the end of the experiment, the mice were sacrificed and tumors and organ tissues were collected. HE staining and immunohistochemistry are serviced by Servicebio. The animal studies were conducted in conformity with institutional guide for the care and use of laboratory animals, and all mouse protocols were approved by the Animal Care and Use Committee of Sichuan University (Chengdu, Sichuan, China).

Acknowledgments

This work was supported by the National Natural Science Foundation of China (81703344), China Postdoctoral Science Foundation (2017M612980), Post-Doctor Research Project, West China Hospital, Sichuan Univeristy (2018HXBH054), and 1.3.5 project for disciplines of excellence, West China Hospital, Sichuan University.

References

[1] M.A. Glozak, N. Sengupta, X. Zhang, E. Seto, Acetylation and deacetylation of non-histone proteins, Gene, 363 (2005) 15-23.

[2] K.J. Falkenberg, R.W. Johnstone, Histone deacetylases and their inhibitors in cancer, neurological diseases and immune disorders, Nat Rev Drug Discov, 13 (2014) 673-691.

[3] A.C. West, R.W. Johnstone, New and emerging HDAC inhibitors for cancer treatment, J Clin Invest, 124 (2014) 30-39.

[4] O. Khan, N.B. La Thangue, HDAC inhibitors in cancer biology: emerging mechanisms and clinical applications, Immunol Cell Biol, 90 (2012) 85-94.

[5] J. Roche, P. Bertrand, Inside HDACs with more selective HDAC inhibitors, Eur J Med Chem, 121 (2016) 451-483.

[6] A. Mai, Small-molecule chromatin-modifying agents: therapeutic applications, Epigenomics, 2 (2010) 307-324.

[7] R. Benedetti, M. Conte, L. Altucci, Targeting Histone Deacetylases in Diseases: Where Are We?, Antioxid Redox Signal, 23 (2015) 99-126.

[8] Q. Wu, W. Li, C. Wang, P. Fan, L. Cao, Z. Wu, F. Wang, Ultradeep Lysine Crotonylome Reveals the Crotonylation Enhancement on Both Histones and Nonhistone Proteins by SAHA Treatment, J Proteome Res, 16 (2017) 3664-3671.

[9] P.A. Marks, R. Breslow, Dimethyl sulfoxide to vorinostat: Development of this histone deacetylase inhibitor as an anticancer drug, Nat Biotechnol, 25 (2007) 84-90.

[10] B.S. Mann, J.R. Johnson, M.H. Cohen, R. Justice, R. Pazdur, FDA approval summary: vorinostat for treatment of advanced primary cutaneous T-cell lymphoma, Oncologist, 12 (2007) 1247-1252.

[11] R. Frye, M. Myers, K.C. Axelrod, E.A. Ness, R.L. Piekarz, S.E. Bates, S. Booher, Romidepsin: a new drug for the treatment of cutaneous T-cell lymphoma, Clin J Oncol Nurs, 16 (2012) 195-204.

[12] H.Z. Lee, V.E. Kwitkowski, P.L. Del Valle, M.S. Ricci, H. Saber, B.A. Habtemariam, J. Bullock, E. Bloomquist, Y. Li Shen, X.H. Chen, J. Brown, N. Mehrotra, S. Dorff, R. Charlab, R.C. Kane, E. Kaminskas, R. Justice, A.T. Farrell, R.

1112 Pazdur, FDA Approval: Belinostat for the Treatment of Patients with Relapsed or
1113 Refractory Peripheral T-cell Lymphoma, Clin Cancer Res, 21 (2015) 2666-2670.
1114 [13] J.P. Laubach, P. Moreau, J.F. San-Miguel, P.G. Richardson, Panobinostat for the
1115 Treatment of Multiple Myeloma, Clin Cancer Res, 21 (2015) 4767-4773.
1116 [14] P.S. Suresh, V.C. Devaraj, N.R. Srinivas, R. Mullangi, Review of bioanalytical
1117 assays for the quantitation of various HDAC inhibitors such as vorinostat, belinostat,
1118 panobinostat, romidepsin and chidamine, Biomed Chromatogr, 31 (2017).
1119 [15] P. Bertrand, Inside HDAC with HDAC inhibitors, Eur J Med Chem, 45 (2010)
1120 2095-2116.
1121 [16] C. Chen, X. Hou, G. Wang, W. Pan, X. Yang, Y. Zhang, H. Fang, Design,
1122 synthesis and biological evaluation of quinoline derivatives as HDAC class I
1123 inhibitors, Eur J Med Chem, 133 (2017) 11-23.
1124 [17] R. Sangwan, R. Rajan, P.K. Mandal, HDAC as onco target: Reviewing the
1125 synthetic approaches with SAR study of their inhibitors, European Journal of
1126 Medicinal Chemistry, 158 (2018) 620-706.
1127 [18] M. New, H. Olzscha, N.B. La Thangue, HDAC inhibitor-based therapies: can we
1128 interpret the code?, Mol. Oncol., 6 (2012) 637-656.
1129 [19] O. Witt, H.E. Deubzer, T. Milde, I. Oehme, HDAC family: What are the cancer
1130 relevant targets?, Cancer Letters, 277 (2009) 8-21.
1131 [20] J.H. Kalin, J.A. Bergman, Development and therapeutic implications of selective
1132 histone deacetylase 6 inhibitors, J. Med. Chem., 56 (2013) 6297-6313.
1133 [21] C. Micelli, G. Rastelli, Histone deacetylases: structural determinants of inhibitor
1134 selectivity, Drug Discov Today, 20 (2015) 718-735.
1135 [22] J. Li, G. Li, W. Xu, Histone deacetylase inhibitors: an attractive strategy for
1136 cancer therapy, Curr Med Chem, 20 (2013) 1858-1886.
1137 [24] R. Sangwan, R. Rajan, P.K. Mandal, HDAC as onco target: Reviewing the
1138 synthetic approaches with SAR study of their inhibitors, European Journal of
1139 Medicinal Chemistry, 158 (2018) 620-706.
1140 [24] K. Vogerl, N. Ong, J. Senger, D. Herp, K. Schmidtkunz, M. Marek, M. Muller, K.
1141 Bartel, T.B. Shaik, N.J. Porter, D. Robaa, D.W. Christianson, C. Romier, W. Sippl, M.

1142 Jung, F. Bracher, Synthesis and Biological Investigation of Phenothiazine-Based
1143 Benzhydroxamic Acids as Selective Histone Deacetylase 6 Inhibitors, J Med Chem,
1144 62 (2019) 1138–1166.
1145 [25] C.W. Yu, P.Y. Hung, H.T. Yang, Y.H. Ho, H.Y. Lai, Y.S. Cheng, J.W. Chern,
1146 Quinazolin-2,4-dione-Based Hydroxamic Acids as Selective Histone Deacetylase-6
1147 Inhibitors for Treatment of Non-Small-Cell Lung Cancer, J Med Chem, 62 (2019)
1148 857-874.
1149 [26] Y. Luan, J. Li, J.A. Bernatchez, R. Li, Kinase and Histone Deacetylase Hybrid
1150 Inhibitors for Cancer Therapy, J Med Chem, 62 (2019) 3171-3183.
1151 [27] H.Y. Lee, S.J. Fan, F.I. Huang, H.Y. Chao, K.C. Hsu, T.E. Lin, T.K. Yeh, M.J. Lai,
1152 Y.H. Li, H.L. Huang, C.R. Yang, J.P. Liou, 5-Aroylindoles Act as Selective Histone
1153 Deacetylase 6 Inhibitors Ameliorating Alzheimer's Disease Phenotypes, J Med Chem,
1154 61 (2018) 7087-7102.
1155 [28] C. Chen, X.B. Hou, G.H. Wang, W.Y. Pan, X.Y. Yang, Y.K. Zhang, H. Fang,
1156 Design, synthesis and biological evaluation of quinoline derivatives as HDAC class I
1157 inhibitors, European Journal of Medicinal Chemistry, 133 (2017) 11-23.
1158 [29] S. Mehndiratta, R.S. Wang, H.L. Huang, C.J. Su, C.M. Hsu, Y.W. Wu, S.L. Pan,
1159 J.P. Liou, 4-Indolyl-N-hydroxyphenylacrylamides as potent HDAC class I and IIB
1160 inhibitors in vitro and in vivo, European Journal of Medicinal Chemistry, 134 (2017)
1161 13-23.
1162 [30] Y. Chen, X. Yuan, W. Zhang, M. Tang, L. Zheng, F. Wang, W. Yan, S. Yang, Y.
1163 Wei, J. He, L. Chen, Discovery of a Novel Dual Histone Deacetylases (HDACs) and
1164 Mammalian Target of Rapamycin (mTOR) Target Inhibitor as a Promising Strategy
1165 for Cancer Therapy, J Med Chem, (2019), DOI: 10.1021/acs.jmedchem.8b01825.
1166 [31] Z. Yang, T. Wang, F. Wang, T. Niu, Z. Liu, X. Chen, C. Long, M. Tang, D. Cao,
1167 X. Wang, W. Xiang, Y. Yi, L. Ma, J. You, L. Chen, Discovery of Selective Histone
1168 Deacetylase 6 Inhibitors Using the Quinazoline as the Cap for the Treatment of
1169 Cancer, J Med Chem, 59 (2016) 1455-1470.
1170 [32] Y. Chen, X. Wang, W. Xiang, L. He, M. Tang, F. Wang, T. Wang, Z. Yang, Y. Yi,
1171 H. Wang, T. Niu, L. Zheng, L. Lei, X. Li, H. Song, L. Chen, Development of

Purine-Based Hydroxamic Acid Derivatives: Potent Histone Deacetylase Inhibitors with Marked in Vitro and in Vivo Antitumor Activities, J Med Chem, 59 (2016) 5488-5504.

[33] S. Valente, D. Trisciuoglio, T. De Luca, A. Nebbioso, D. Labella, A. Lenoci, C. Bigogno, G. Dondio, M. Miceli, G. Brosch, D. Del Bufalo, L. Altucci, A. Mai, 1,3,4-Oxadiazole-containing histone deacetylase inhibitors: anticancer activities in cancer cells, J Med Chem, 57 (2014) 6259-6265.

[34] Y. Miyake, J.J. Keusch, L. Wang, M. Saito, D. Hess, X. Wang, B.J. Melancon, P. Helquist, H. Gut, P. Matthias, Structural insights into HDAC6 tubulin deacetylation and its selective inhibition, Nat Chem Biol, 12 (2016) 748-754.

[35] Y. Hai, D.W. Christianson, Histone deacetylase 6 structure and molecular basis of catalysis and inhibition, Nat Chem Biol, 12 (2016) 741-747.

[36] P.J. Watson, C.J. Millard, A.M. Riley, N.S. Robertson, L.C. Wright, H.Y. Godage, S.M. Cowley, A.G. Jamieson, B.V. Potter, J.W. Schwabe, Insights into the activation mechanism of class I HDAC complexes by inositol phosphates, Nat Commun, 7 (2016) 11262.

[37] J. Pottel, E. Therrien, J.L. Gleason, N. Moitessier, Docking ligands into flexible and solvated macromolecules. 6. Development and application to the docking of HDACs and other zinc metalloenzymes inhibitors, J. Chem. Inf. Model, 54 (2014) 254-265.

[38] K. Cheng, S. Li, C. Liao, Progress in the Discovery of Macrocyclic Histone Deacetylase Inhibitors for the Treatment of Cancer, Curr. Med. Chem., 24 (2017) 4166-4179.

- 1,2,4-Oxadiazole-Containing Selective Histone Deacetylase Inhibitors
- Nanomole antiproliferative activities in a panel of cancer cell lines
- Inducing cell cycle arresting at G1 phase and apoptotic effects
- Oral bioavailability was up to 53.52%